Predictive Temperature and Humidity Control in Integrated Building Energy Management Systems

Andrea Carlota Díaz Guasgua

Master of Science Thesis

TU Delft Delft University of Technology

Delft Center for Systems and Control

Predictive Temperature and Humidity Control in Integrated Building Energy Management Systems

Master of Science Thesis

For the degree of Master of Science in Systems and Control at Delft University of Technology

Andrea Carlota Díaz Guasgua

July 1, 2019

Faculty of Mechanical, Maritime and Materials Engineering (3mE) · Delft University of Technology

Delft University of Technology
Department of
Delft Center for Systems and Control (dcsc)

The undersigned hereby certify that they have read and recommend to the Faculty of Mechanical, Maritime and Materials Engineering (3mE) for acceptance a thesis entitled

Predictive Temperature and Humidity Control in Integrated Building Energy Management Systems

by

Andrea Carlota Díaz Guasgua

in partial fulfillment of the requirements for the degree of

Master of Science Systems and Control

Dated: July 1, 2019

Supervisor(s):

Dr.ir. Tamás Keviczky

Reader(s):

Prof.dr. Laure Itard

Dr.ir. Arman Sharifi Kolarijani

Prof.dr.ir. Jan H. van Schuppen

Ir. Yvo Putter

Abstract

Worldwide roughly 80% of heating and cooling systems in the building sector are currently dominated by fossil-fuel technologies, [1]. These systems, known as Heating, Ventilation and Air Conditioning (HVAC) systems in buildings, are key drivers of global energy consumption growth, and they have caused detrimental effects to the environment as well as considerable operational costs to the owners. These effects are mainly the consequence of the increasing demand of HVAC systems over the last decades due to population growth, and improved building climate comfort and indoor environmental quality requirements. Moreover, the use of fossil-fuel based systems has contributed and will contribute to global climate change, and thus, global warming, greenhouses emissions and weather variations.

To reduce and in an attempt to mitigate the aforementioned effects, the European Union established the Performance of Building Directive (EPBD) that requires "all new built buildings to be nearly zero energy buildings by 2020" and old ones will need to comply this regulation by 2050, [2]. This has motivated the improvement of heating and cooling systems of buildings, for instance by replacing their system components for energy efficient systems or implementing better control strategies. These improvements cause not only environmental benefits, but also the potential to realize savings. In this thesis project, our focus is on the implementation of advanced control strategies.

The control of HVAC systems in buildings aims to provide thermal comfort and acceptable indoor air quality. These factors are influenced by temperature, humidity and CO_2 emissions. While we will not discuss the influence of the CO_2 in this project, it is important to note that the air quality is highly affected by it. Thermal comfort and indoor air quality together with the reduction in energy consumption is the core of this work, we propose a nonlinear Model Predictive Control (MPC) as an approach to solve the temperature and humidity control while aiming to realize energy consumption reduction in buildings.

MPC has been identified as an optimal control strategy, since it offers the possibility to express the problem as an optimization program with constraints over a prediction horizon. Here, the major advantage of using MPC in comparison to classic control methods for building climate comfort is the straightforward relation between temperature and humidity to energy consumption, which is quantified in the objective function definition. In this project, we use

a nonlinear MPC to solve the cooling and dehumidification problem of a building, which we represent as a mathematical model of a single zone space using the thermodynamics laws of energy and mass conservation. We consider the case in which a cooling coil dehumidifies the air, and a heating coil re-heats the air. Their dynamics are indirectly integrated in the MPC formulation by analyzing the air conditioning processes of the air across the coils. These processes are graphically represented in the psychrometric chart. That allows us to define the overall system's enthalpy or total heat content balance as the vector between the mixed air and supply air temperatures and humidity ratios. This vector is integrated into the objective function definition in the MPC formulation.

The problem formulation of the MPC is defined by the reference tracking of the temperature and humidity ratio in the zone and the energy minimization problem, which corresponds to a nonlinear constrained optimization problem. Here, the constraints are described by the system dynamics of the temperature and humidity ratio of the zone, states constraints, and the input constraints. The inputs correspond to the temperature and humidity ratio of the supply air. In this formulation, the state constraints and the reference tracking allow to indirectly limit the evolution of the relative humidity in the zone. The energy minimization problem corresponds to one of the following cases, the optimization with respect to the (i) air mass flow rate, (ii) the air mass flow rate and the sensible heat from ventilation and (iii) the air mass flow rate and the enthalpy vector.

We investigate the opportunity to improve the energy efficiency by providing an analysis of the aforementioned scenarios. From which the first was taken as the reference controller. To solve the nonlinear program, we use the toolbox Yalmip and the Sequential Quadratic Programming (SQP) solver. The toolbox supplies the warm-starting for the optimization problem inside the bounds defined so that the problem is feasible, and then it computes the solution. The results from these approaches confirm comfort requirements. And they also show that case (iii) provides the least energy consumption in comparison to (i) and (ii).

Table of Contents

List of Figures

List of Tables

Acknowledgements

I would like to express my gratitude to my supervisor Dr.ir. Tamás Keviczky and Prof.dr.ir. Jan H. van Schuppen for their assistance during the writing and development of this thesis. Your guidance and the freedom to explore the project from different perspectives allowed me to build my knowledge in the topic.

My sincere thanks to Ir. Yvo Putter for the fruitful discussions we had and the general insights he gave me regarding the thesis project itself. Also, I would like thank my friends, and in particular a very special thank you to Martin Bauer.

Last but not least, I would like to thank my family for always supporting me throughout my life.

Delft, University of Technology
July 1, 2019

Andrea Carlota Díaz Guasgua

In dedication to my beloved family.

Your support, encouragement and advice have served me as inspiration to achieve this milestone in my life of receiving the degree of Master of Science in Systems and Control.

There are no words to express my utmost affection and gratitude. These lines are my humble way to show it.

Chapter 1

Introduction

This chapter gives an overview of MPC control of HVAC systems in buildings for climate comfort with focus on cooling and dehumidification by means of cooling and heating coils. This topic is motivated by the necessity to reduce energy consumption, achieve economical savings and lessen environmental side effects. Herein, climate comfort is analyzed by the dynamic behavior of the temperature and humidity in the building. The impact of these variables to maintain a comfortable environment in an energy-efficient manner is explored by MPC. To build a better understanding of the HVAC system under study, the first section introduces its relevant concepts and the challenges between achieving climate comfort and an energy efficient operation of the system. Then, we present relevant literature to this work, which is followed by the contribution of this thesis. Finally, we end this chapter with the report structure and an outline of each of the following chapters.

1-1 Background

In the building sector to help mitigate the effects of climate change and also to decrease operational costs, it is necessary to execute efficient operations of the HVAC system while guaranteeing thermal comfort and air quality. These conditions are mainly influenced by temperature and humidity, where humidity is explained as relative and specific humidity (humidity ratio). An appropriate level of these variables reduces the side effects on occupants, equipment, building materials and in general on items sensitive to temperature and humidity fluctuations. For instance, poor indoor climate conditions negatively affect the productivity and efficiency of people, and they induce a faster rate of deterioration or even malfunctioning on materials and equipment. Hence, the main goal of the HVAC system is to comply with the climate comfort requirements while avoiding those undesired effects.

1-1-1 HVAC systems - A brief overview

In current practices, Heating, Ventilation and Air Conditioning (HVAC) systems in buildings are controlled by conventional control such as rule based methods and PI controllers. The

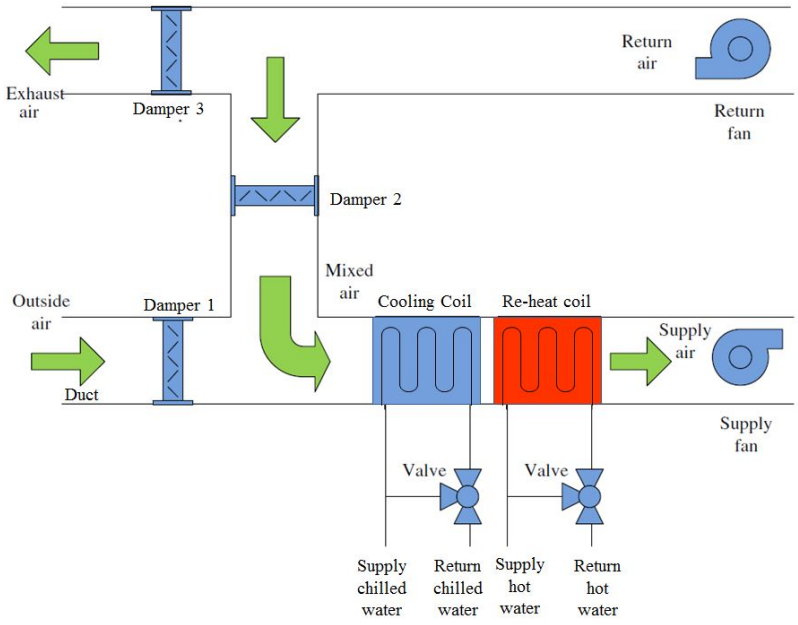

Figure 1-1: Schematic diagram of an HVAC system for cooling and dehumidification, adapted from [3]

energy consumption of the HVAC equipment is commonly administered by the Building Energy Management System (BEMS), where their set-points are configured. The classic control rules are easy to implement while attaining the desired comfort requirements. However, an energy efficient operation is not guaranteed and its tuning relies on the expertise of the designer. Also, since the relation of the variation of set-points and the energy consumption is not straightforwardly linked, the classic control rules become harder to manipulate. Manipulation that can be further hampered when not only human comfort must be achieved, but also material comfort. For instance, in museums, hospitals or libraries.

In small to medium -size buildings and even some large-scale buildings, temperature and humidity are jointly controlled, [9]. Even though a potential solution is the migration to dedicated equipment that independently control these variables, its implementation is hampered for instance by economical aspects or lack of space in the building. In these scenarios, the HVAC system performs the climate control by conditioning the outside air by means of its components, such as dampers, coils, and fans. In this air conditioning cycle, the most expensive process in terms of energy usage is cooling and dehumidification. Thus, for these systems there still exists the need to control temperature and humidity jointly.

The HVAC system being investigated is shown in Figure 2-1. This system controls the temperature and humidity inside a room by conditioning the outside air and distributing the treated air to the room, Figure 1-2. The supply fan transports the outside air into the duct, where damper 1 determines the quantity of fresh to pass. Then, this air is mixed with an amount of the return air from the room determined by damper 2. This mixture is then cooled and dehumidified in the cooling coil. The process that occurs through this coil is the heat interchange between the chilled water from the production units and the air. This preconditioned air is then re-heated in the heating coil (re-heat coil) by exchanging heat

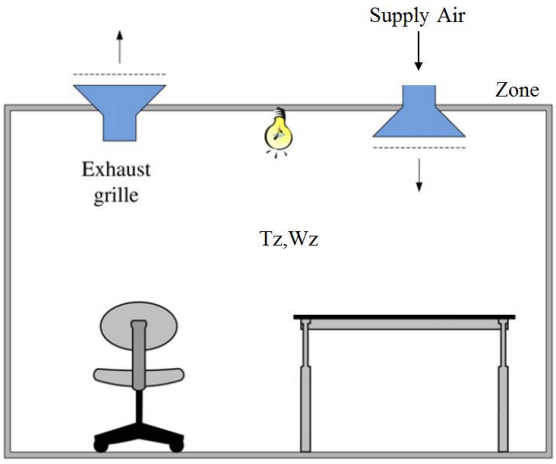

Figure 1-2: Schematic of the ventilating system of a room, adapted from [3]

between the air across the coil and the hot water from the production units. This conditioned air is delivered to a room or space, referred to as zone, to control the temperature T_z and the humidity ratio W_z therein, Figure 1-2. A return fan transports the air out from the room through an exhaust grille so that the air is continuously circulating. A portion of this air is returned to the space while the rest is exhausted to the environment by the position of dampers 2 and 3, respectively. These processes correspond to the air conditioning cycle that controls temperature and humidity inside the building.

The understanding of the air conditioning process is a key aspect in the control of temperature and humidity, especially with regard to humidity. At the room level, moisture changes occur due to the air movement and exogenous inputs. For instance, the former caused by the air mass flow rate produced by the fans, and the latter by occupancy or outside infiltration air. In our system we consider occupancy as the only moisture gain in the building, however, other moisture sources such as infiltration produced by cracks in the building envelope or the opening of doors and windows may have considerable effects on the humidity. Consequently, the humidity ratio variation in the room is the result of the interaction of the aforementioned exogenous inputs and the air conditions from the ventilation of the supply air.

The supply air conditions from ventilation are the result of the dehumidification and re-heating processes through the heating and cooling coils. These conditions allow to control the temperature and humidity in the building and the heat being transferred to the zone is produced by the air mass flow. Here, the fan produces the air mass flow rate that transports the conditioned air throughout the room, thus it transfers latent or sensible heat to the room. The latent heat from ventilation corresponds to a moisture input controlled by the HVAC system and may negatively affect the humidity ratio inside the room if the conditioned air has less moisture than the internal moisture generators. If dehumidification is required in the building, the amount of moisture from ventilation injected into the zone is the result of the dehumidification of the mixed air across the cooling coil. Otherwise, it is the result of the mixed-air conditions. The supply air temperature from ventilation is produced by either the cooling or heating coils, in which the heating coil does not affect the cooling off-coil humidity ratio.

1-1-2 Challenges of temperature and humidity control

In this work, the problem that we aim to solve is determining the optimal temperature and humidity in terms of energy efficiency of the air conditioning equipment, namely the cooling and re-heat coils. There are identified two factors influencing the complexity of the problem, which are its modeling and the controller synthesis of the joint control of these variables.

HVAC systems in building modeling poses as complex, nonlinear, discrete-time Multiple-Input Multiple-Output (MIMO) systems, [3]. For the sake of simplicity, we assume a mathematical model of a building where the parameters of the system are known. However, this assumption will need to be further investigated in a separate project by system identification and filtering techniques. Even though the parameters in this work are assumed to be known, the nonlinearities yield higher computational effort and tractability issues when an advanced controller, namely MPC, is implemented.

To overcome the aforementioned issues, the simplification of the system dynamics is required. This is possible to realize by the understanding of the air conditioning processes, which are better explained by psychrometrics, the studies of the properties of the air. Regarding the humidity property of the air, the distinction between humidity ratio and relative humidity is a key aspect to the zone model, since the humidity ratio variation in the zone can be considered to be decoupled from the temperature in the zone. This no longer holds for the relative humidity, because it shows a nonlinear coupled relation with the temperature and humidity ratio. These psychrometric concepts allow us to model the dynamics of the temperature and humidity ratio in the zone as a nonlinear system, and disregard the coils dynamics. Thus, the complexity of the system is reduced and the model captures the air conditioning processes, which corresponds to the change of phase of the air. This process starts when the air is transported from the inlet damper, distributed and conditioned by the cooling and re-heat coils to the room and returned or exhausted from or out of the system by the respective dampers.

Temperature and humidity regulation in buildings is determined by the operation of the HVAC system equipment, their controllers, and the operational set-points during each season of the year. We assume that low-level controllers exist that are able to track the set-points, and we define the scope of the project to a time period when cooling and dehumidifying of the air is needed. Herein, the set-points relation to energy is not a straightforward concept, and their operation is not guaranteed to be energy efficient. To define this relation, Model Predictive Control (MPC) is able to address the minimization of energy consumption and maximization of comfort as an objective function, while also handling the constraints for climate comfort. For instance, by limiting the temperature, humidity ratio, and the conditioned air inputs in a specific range. By limiting the temperature and humidity ratio in the zone, we are able to limit the relative humidity. The challenge of implementing MPC arises from the modeling itself, the availability of forecasts of the pertinent exogenous variables, and the existence of a solution to the nonlinear optimization problem.

Modeling, as explained earlier, yields a nonlinear discrete time MIMO system of the room. Here, the computational effort is the main burden, however, the nonlinear program is still tractable with respect to the slow dynamics of temperature and humidity. It is desirable that the problem yields a convex formulation for faster convergence. Regarding the forecast, which in this particular case are the predictions of the weather and occupancy, the data is

considered to be deterministic and given. Ideally this might not be case, and data should rather be collected over a representative period of time. Finally, as the problem is posed as a nonlinear programming, the numerical method to solve the optimization should be able to provide a solution within the defined sampling time.

1-2 Related work

In the building sector, the control strategy algorithms have experienced a slow evolution over the last decades, [10]. This is evidenced by the considerable amount of studies that have only dealt with the control of HVAC systems for temperature regulation and have partly covered other factors such as humidity. A brief overview of the most relevant studies that address MPC in HVAC systems in buildings will be presented next.

A MPC for temperature regulation in large-scale buildings was proposed in [11]. This work used a distributed control to solve two problems formulated from the water-side and the air side subsystems of the HVAC system. The former problem was expressed as a high-level optimization problem of the whole building, and the latter as a low-level optimization problem in each room. Both problems sought to optimize the energy used to reach the defined comfort temperature. This architecture allowed to formulate the solution of the high-level controller as constraints in the low-level problem. Here, the dynamics of the overall temperature of the building and rooms were represented by linear models. This simplification may no longer be applicable when the humidity dynamics are considered.

In [12] a nonlinear MPC was proposed for temperature regulation of a multi-zone building for energy consumption reduction and a similar study was found in [13]. The main consumers from the HVAC system corresponded to a cooling coil and a fan, in which each room had its own VAV box to control the air flow rate. In [12] the cooling coil energy calculation in the optimization problem followed the sole interaction of the supply air temperature with the room temperature, however, this assumption does not hold if we further analyze the air conditioning processes. A similar calculation was found in [14]. The relevance of the nonlinear formulation is in posing a modeling technique that could cope with the inclusion of humidity.

The studies from [15, 16, 17] addressed the control of the HVAC of temperature and humidity regulation in a space. These approaches use a linear system of the dynamics of the air conditioning units and the room. [15] presents a practical implementation in which the model parameters of the linearized system are updated at each sampling time, providing a solution to deal with the nonlinearities of the plant. A similar approach followed [16], where a priory optimization steered the system to an optimal steady-state while minimizing energy consumption. The drawback of these studies is when the disturbances are considerably large, the system could be steered out of the neighborhood of the operating point.

Studies addressing temperature and humidity control with advanced control strategies were found in [18, 19], and even though the object of control was a greenhouse, the controller used were MPC. In [18], the problem was cast as a multi-objective problem, which was solved using game-theory. Here, the modeling was carried out by system and identification techniques, thus, confirming that one of the challenges for MPC is the modeling of the system. In [19], a detailed mathematical modeling and its validation of the system was carried out. This model laid the basis of the nonlinear MPC. The optimization problem used a grid-search

for the warm-starting, and the results assessed a considerable improvement with respect to the conventional control of the greenhouse.

To the best knowledge of the author of this thesis, the air-conditioning process that experiences the air throughout the HVAC system has not been explained in detail in the literature found of MPC and HVAC systems for temperature and humidity control of buildings. The most relevant study found was from the air conditioning of a car, [20, 14]. This research provided a detailed explanation of the phase change of the air using the standard psychrometric chart. The analyzes enabled the calculation of the system inputs, in which no optimization was carried out. The results from this study showed that this approach performs better than a fuzzy controller for temperature and humidity regulation. Although this study is not directly related to building energy comfort, it provides enough tools to understand the cycle of the air conditioning process to offset temperature and humidity.

1-3 Contribution

We developed a simplified representation and of an HVAC system in a building for cooling and dehumidification. This development mainly differs from literature by the analysis of the psychrometrics of the air. From this study, we identified that dehumidification is produced by the cooling coil after the dew-point temperature has been reached, and that the temperature variation produced by the cooling or heating coils does not change the phase of the air for temperatures higher than the dew-point. We used these findings to establish the simplified model, which accounts only to the building dynamics. This model indirectly relates to the cooling and heating coils by the supply air temperature and humidity ratio, which are considered as inputs together with the air mass flow rate. Also, the psychrometric chart allowed us to determine the enthalpy vector of the system as the vector between the mixed air and supply air conditions.

The simplified model described by the dynamics of the building and the enthalpy vector of the HVAC system in the building were used in the problem formulation of the MPC. Herein, the heating and cooling coil dynamics were not necessary since they were integrated by the temperature and humidity ratio of the supply air as decision variables. We assumed the existence of low-level controllers to track those variables. By means of the MPC capability to pose the problem as an optimization algorithm, we included the enthalpy vector in the cost function and solved the problem with the constraints on the states and inputs. Although the system is nonlinear, the computational effort and complexity of the optimization problem was considerably reduced by disregarding the dynamics of the coils.

We also provided an analysis of the MPC control strategy of a simple case of study in a mild summer day. We discussed reducing the heat produced by the coils by defining a cost function for reference tracking of the temperature and humidity ratio and the energy consumption in the building. Herein, three scenarios were discussed that differ in the energy consumption cost. This cost corresponded to the air mass flow rate, the sensible heat from ventilation and the enthalpy of the system. We also compared the difference between the sensible heat from ventilation injected to the building and the total heat required by the coils during cooling, cooling and dehumidification or heating. We developed this analysis to show that the heat load of the coils is not the heat injected to the system from ventilation, especially during the

dehumidification periods. This demonstrated that for temperature and humidity control, the thermal heat profile of a building has to take into account the air conditioning processes of the air throughout the components of the HVAC system.

1-4 Report Structure

The content of this report have been structured in four chapters. This introductory chapter explains the motivation, related work and contribution of this thesis, and the following chapters are described in the next paragraphs.

Chapter 2 describes the HVAC system for cooling and dehumidification of a space and its mathematical modeling. The components are briefly described with relevance to the control problem definition. This is followed by the analysis of the air conditioning processes by means of the psychrometric chart, which allows us to clearly visualize the phase changes of the air. These concepts lay the basis of the system modeling and its simplification, which is presented next together with the additional modeling considerations.

Chapter 3 presents the proposed controller for the system that corresponds to a nonlinear Model Predictive Control (MPC). It discusses the problem formulation for the MPC, its objective function, constraints and assumptions. Prior to developing the numerical studies, we discuss the effects on the humidity ratio when we control only the temperature and the system has considerable moisture gains. After, we present the joint control by MPC of the temperature and humidity ratio of an academic model of a building. The numerical examples analyzed differ from each other on the cost function, which is defined by the air mass flow rate, the sensible heat from ventilation and the enthalpy of the system as the energy optimization term.

Chapter 4 is the final chapter of this work, and it outlines our conclusions and recommendations for future work.

To conclude this report, we present the supporting information of this thesis. These sections explain concepts used throughout this report: the psychrometrics of the moist air, the fundamentals of MPC and the parameters and constants used for the numerical example from Chapter 3.

Chapter 2

System description and modeling

This chapter describes the HVAC system for cooling and dehumidification and its modeling oriented to model-based control. Section 2-1 introduces the heat transfer phenomena that affects the inside temperature and humidity ratio of buildings. Section 2-2 describes the components of the system, in which we analyze the air conditioning process of each. The understanding of these processes is presented in Section 2-3 by using psychrometrics. We finish this chapter with Section 2-4, where we present the mathematical model of the system. Throughout this and the following chapter the notation from Table 2-1 is used.

2-1 Heat transfer in buildings

The mechanisms for the generation, use, conversion and exchange of heat between the building, the HVAC system, and its surrounding physical systems rely on thermodynamics and mass conservation laws. Herein, we support our study with the fundamental principles of the first law of thermodynamics. This principle states that the heat change of the system's energy is equal to the energy transferred by heat and work, which is a formulation of the energy conservation law. Similarly, the mass conservation law states matter cannot be created or destroyed, but it can change forms, [21]. In general, the mechanisms for heat transfer can be either sensible or latent.

2-1-1 Sensible heat transfer

It describes the heat exchange of a thermodynamic system, namely a gas or an object, while there exists a variation in its temperature without affecting its phase. Herein, sensible heat is associated to the thermal energy that is required to change the temperature of the thermodynamic system. Mathematically, the sensible heat $\dot{Q}$ can be expressed as:

$$\dot{Q} = cm\Delta T, \tag{2-1}$$

Table 2-1: Notation

Symbol	Description
T	Temperature
W	Humidity ratio
$\dot{Q}$	Heat transfer rate
Q	Heat energy
h	Enthalpy
q	Heat Flux
$\dot{m}$	Mass flow rate
c_{a}	Specific heat coefficient of air
h_{wv}	Latent heat of vaporization of water vapor
ρ	Density
V	Volume
A	Area
C	Thermal capacitance
U	Thermal transmittance

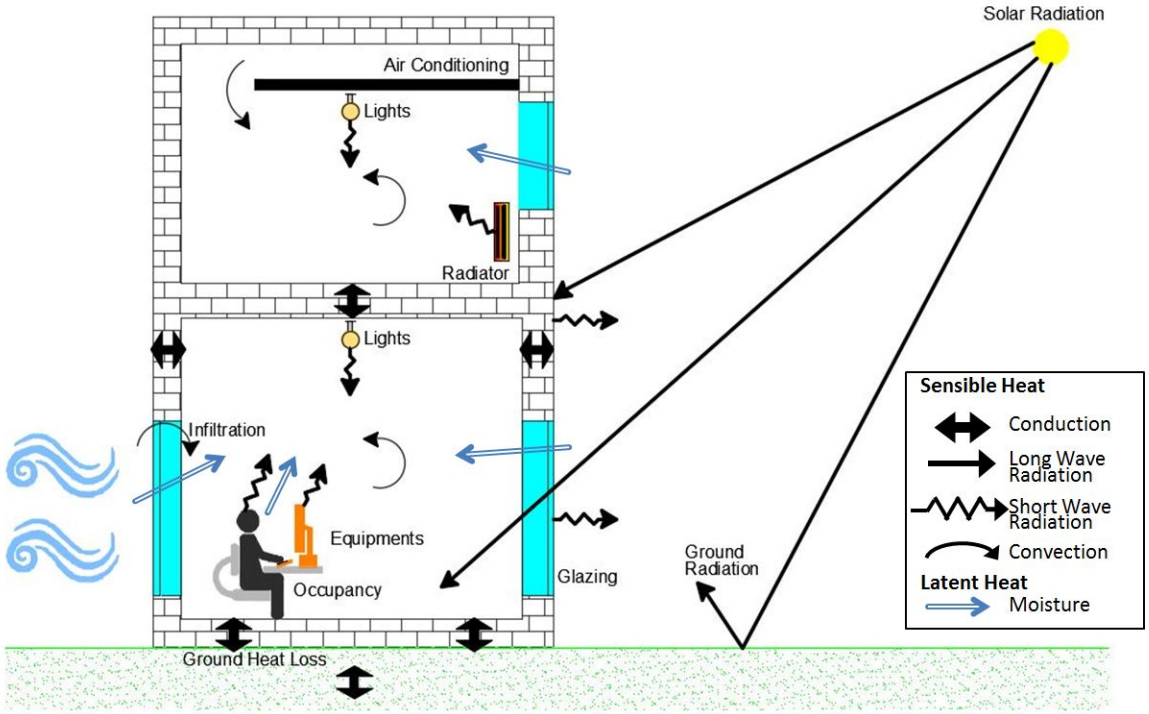

Figure 2-1: Heat Transfer Mechanisms in Buildings, adapted from [4]

where c is the specific heat of the material, m the mass of the gas or object and ΔT the change in temperature. The thermodynamic system can either absorb or give-off thermal energy in an amount that depends on the material specific heat. Moreover, the heat transfer is unidirectional from the hotter system to the cooler system, and is the result of conduction, convection or radiation acting alone or in combination.

- **Conduction**
  It occurs by diffusion of the internal heat within the body as a result of a temperature difference across of it. In buildings, this phenomenon can be evidenced in the temperature difference of walls or windows produced by the outside and inside space temperatures. This heat transfer in the envelope is particularly important for the heating or cooling losses to the outside and for the operational costs related to it. Herein, the conductivity of building materials is expressed by the U-value, which is a quantification of its insulation effect.

- **Convection**
  It is the heat transfer within a fluid such as a gas or liquid that results from the fluid movement across a surface. It is related to "the fluid transport properties (specific heat, viscosity, thermal conductivity and density), fluid velocity and the geometrical relationship between surface and fluid flow", [22]. Convective heat transfers relevant to buildings are related to the wind, forced air movement, or space heating or cooling by fluid movement. For instance, the natural ventilation by the wind, the forced air movement by fans and the fluid movement in coils, radiators or convectors.

- **Radiation**
  It occurs due to electromagnetic waves through gas or vacuum, which means that radiation does not require a fluid medium to transfer heat but rather an air gap. Radiation is affected by the reflectivity and emissivity properties of a surface. The former property determines the reflected radiation from a surface, and the latter the capacity of a body to emit radiation. They also vary depending on the wavelength of the radiation. With relevance to buildings, the heat exchange in its surfaces is related to long- and short-wavelength radiation transfers. In which, the emitter sources differ from each other by the amount of heat they produce. Examples of those emitters are the sun as long-wave emitter, and people, equipment, and lighting as short-wave emitters, [23].

An example of these three phenomena is shown in Figure 2-1. Here, the sun transmits heat by radiation to the earth and the surfaces of the building such as walls and glazing. This heat can be either absorbed by conduction or reflected as radiating heat to the environment. Inside the building, this heat is transferred to the indoor air by convection, for instance from the air movement caused by the air conditioning system.

2-1-2 Latent heat transfer

Latent heat is related to the variation in the humidity ratio of the air, and it is related to the amount of heat required to change the phase of the air whether for dehumidifying or humidifying the air. These processes correspond to the condensation of the water vapor in the air, and the evaporation of water into water vapor, respectively. The energy required to

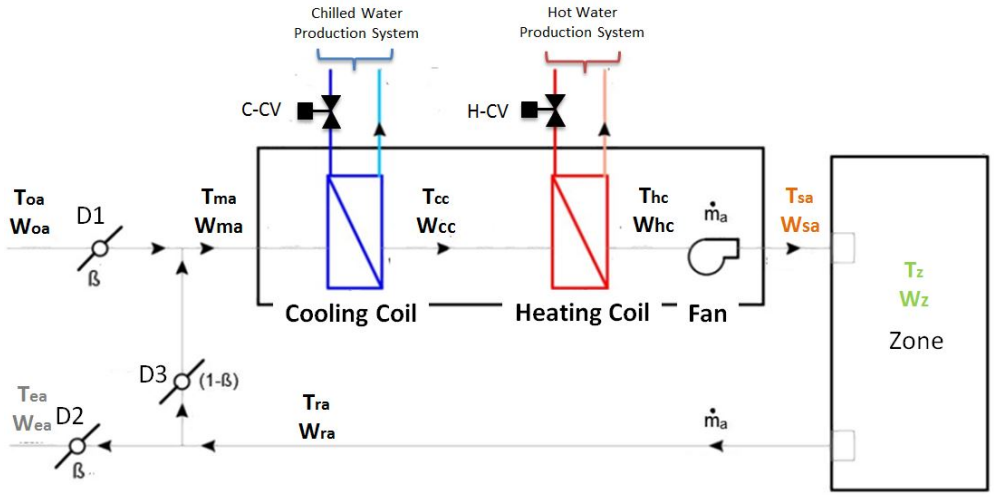

Figure 2-2: Components of the studied HVAC system

change the phase of the air amount to substantial heat losses for instance the heat required to evaporate 1 kg water is 2500 kJ, [24].

As shown in Figure 2-1, occupancy adds moisture to the air causing an increase of the building humidity ratio, similarly, the infiltration air from the outside weather conditions. This latent heat corresponds to a certain amount of energy to dehumidify the air inside this building, which is provided by the air conditioning system.

2-2 Components of the HVAC system

The components of the air conditioning system of the building discussed in this project are shown in Figure 2-2. We consider the building to be an abstraction represented by one single-zone space. A single zone-space is a cluster of offices, heat transmitters and emitters where the temperature and humidity fluctuations are the result of the phenomena explained in Section 2-1. To control these variables, the HVAC system adds or removes latent or sensible heat, in which each component has a role in the air conditioning process, which is explained next.

Dampers

The dampers ($D_1, D_2,$ and D_3) distributes the air through the ducts in and out of the zone. D_1 is the damper of the outside weather conditions, namely temperature T_{oa} and humidity ratio W_{oa}. The β factor corresponds to the amount of fresh air inlet into the building. D_2 is the damper of the exhausted air to the exterior of the building, where the air has a temperature T_{ea} and humidity ratio W_{ea}. D_3 is the return damper that controls the amount of return air from the zone, where the air has a temperature T_{ra} and humidity ratio W_{ra}. The factor $1-\beta$ corresponds to the amount of return air from the zone that is mixed with the outside air.

Fan

The air mass flow rate $\dot{m}$, produced by the fan, transports the air from the exterior into the building and back. It delivers the conditioned air that has a temperature T_{sa} and humidity ratio W_{sa}, which is capable to offset the zone temperature T_{z} and humidity ratio W_{z} by ventilation. Ventilation transports the moisture throughout the zone. While it provides a humidity ratio W_{sa} less than the latent heat gains, the humidity ratio in the zone W_{z} decreases. In contrast, a positive contribution by the humidity ratio from the supply air W_{sa} increases the humidity ratio in the zone W_{z}. This variation in moisture is the consequence of the mass conservation principles.

Heating and cooling coils

The air conditioning occurs in the heating and cooling coils, where the temperature and humidity ratio T_{cc}, T_{hc}, W_{cc} and W_{hc} are the result of the convective heat interchange between the water from the production units and the air in each coil. The water that flows through each coil is controlled by a chilled water controlled valve $C-CV$ and a hot water controlled valve $H-CV$.

The cooling coil reduces the air temperature, and under certain conditions condensates the water vapor of the moist air. This condensation process causes a decrease in the humidity ratio of the mixed air. This change of phase of the air occurs when the off-coil temperature has reached values below the dew-point temperature of the mixed air. The amount of dehumidification required is related to the zone comfort conditions.

The heating coil role is to increase the temperature of the air after the cooling coil. In this system it is considered to be a re-heat element. Whenever the temperatures produced by dehumidification are below an acceptable temperature, re-heating the air is necessary; an acceptable supply air temperature is between 12 [°C] and 24 [°C]. Increasing the air temperature does not affect the humidity ratio.

The aforementioned components keep the zone under comfortable settings by means of circulating conditioned air to the zone. This conditioned air is the result of mixing the outside air (T_{oa}, W_{oa}) and return air (T_{ra},W_{ra}) from the zone in a proportion β given by the dampers positions (D_1, D_2 and D_3). Then, this mixed air (T_{ma},W_{ma}) is dehumidified in the cooling coil resulting in a preconditioned air (T_{cc},W_{cc}). Later, the air is re-heated again (T_{cc},W_{cc}), which corresponds to the actual conditioned air (T_{sa}, W_{sa}) delivered to the zone.

2-3 Air conditioning - A psychrometric analysis

To support the processes in each component of the HVAC system explained in Section 2-2, the psychrometry for the complete air conditioning system can be developed to deploy a graphical analysis in the psychrometric chart. In HVAC systems, it is a common practice to use psychrometrics to analyze moist air. Its properties and processes are represented by its sensible and latent heat balance, which can be graphically visualized with the aid of the psychrometric chart, [25]. Refer to Appendix A for the description and concepts used in this section.

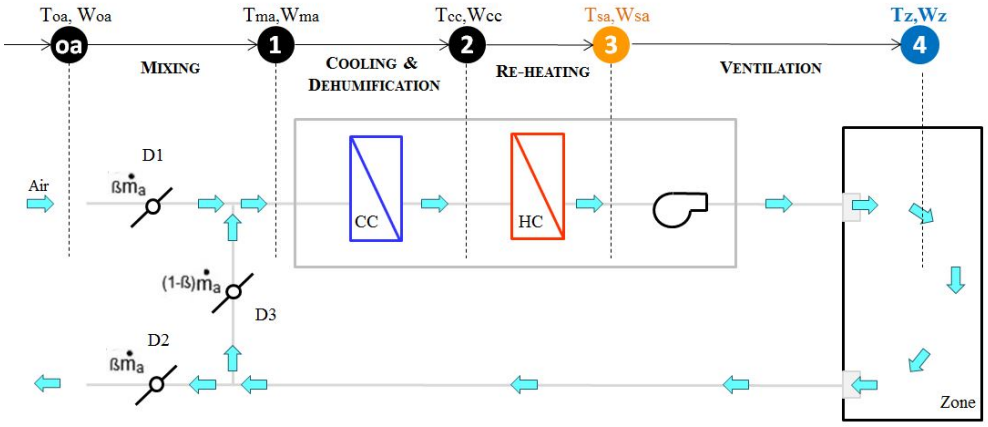

Figure 2-3: Cooling and dehumidification scheme of the system

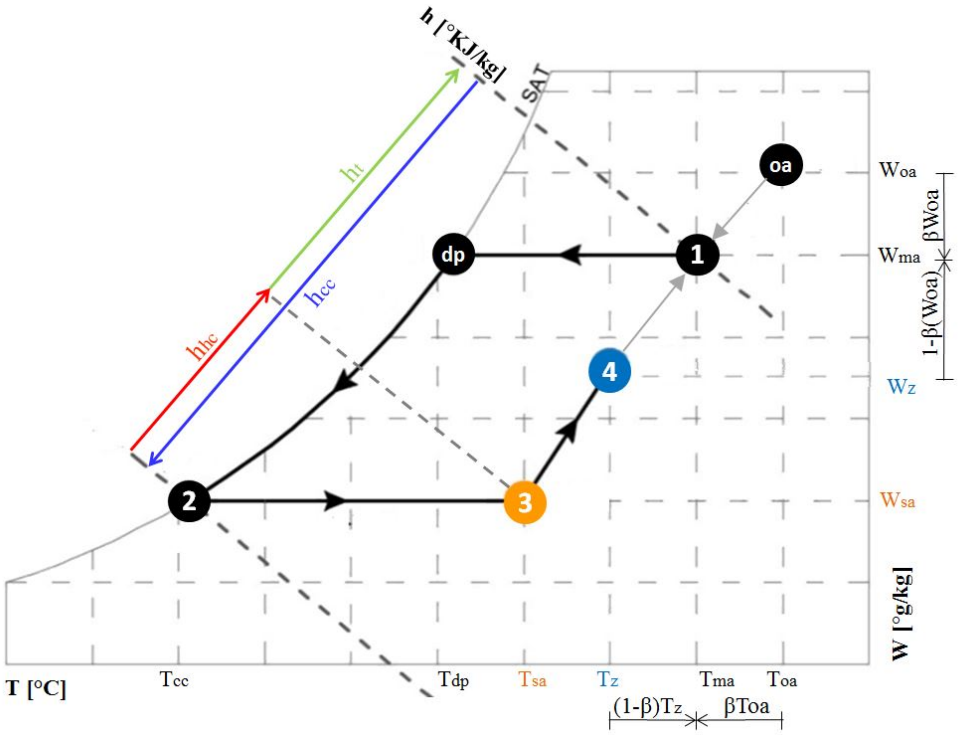

Figure 2-4: Psychrometric process for energy balance of the system

Regarding to our case of study the processes of cooling, dehumidification, heating and ventilation are represented in the figures 2-3 and 2-4. Figure 2-3 shows the air distribution in each component and Figure 2-4 the complementary psychrometric processes associated to each of these components.

2-3-1 Mixing process

It corresponds to the process of mixing the outside air **point oa** and the return air **point 4** resulting in the conditions of **point 1** by means of the dampers D_1, D_2, and D_3. Wherein, it is assumed a perfect mixture and an ideal gas behavior. Then, it follows that the outside temperature T_{oa} and humidity ratio W_{oa} mix with the return air conditions. These conditions are defined by the temperature T_{ra} and humidity ratio W_{ra} of the return air, which are considered to be equal to the temperature T_{z} and humidity ratio W_{z} of the zone. The proportion of the mixture is given by the factor β that determines the amount of fresh air drawn into the building. In Figure 2-4 this mixture corresponds to the **point 1**, where the air has a temperature denoted by T_{ma} and a humidity ratio denoted by W_{ma}.

$$T_{\text{ma}} = \beta T_{\text{oa}} + (1-\beta) T_{\text{z}} \tag{2-2a}$$

$$W_{\text{ma}} = \beta W_{\text{oa}} + (1-\beta) W_{\text{z}} \tag{2-2b}$$

2-3-2 Cooling and dehumidification process

This process occurs as the mixed air at **point 1** pass through the cooling coil CC until reaching the off-coil conditions of **point 2**, Figure 2-3. The air from **point 1** comes in contact with the cooling coil surface and interchanges heat with the chilled water in the tubes. If this heat interchange produces an off-coil temperature T_{cc} below the dew-point temperature T_{dp}, which lies in the saturation line (Relative Humidity 100%), the water vapor in the air partly changes its phase from vapor to water. In Figure 2-4, this is visualized with the arrows indicating a decrease in temperature from **point 1** to **point dp**, where no change of phase of air exists. A further decrease in temperature causes a decrease in the humidity ratio until **point 2** as the air is still saturated. Denote at point 2 the air temperature by T_{cc} and the humidity ratio by W_{cc}.

2-3-3 Re-heating process

This process occurs as the off cooling coil air at **point 2** passes through the heating coil HC until reaching the supply air conditions of **point 3**, Figure 2-3. The air from **point 2** traveling across the coil interchanges heat with the hot water in the tubes of the coil thus increasing the off coil air temperature. In Figure 2-4, this is visualized with the arrows indicating an increase in temperature from **point 2** to **3** while the humidity ratio remains unchanged. At **point 3**, the temperature T_{sa} and humidity ratio W_{sa} of the supply air are equal to the temperature T_{hc} and the humidity ratio W_{hc} at the outlet of the heating coil

This heating stage is known as a re-heating process, and it is a necessary process that counteracts the low temperatures that may be produced by the cooling coil when dehumidification is needed. These low temperatures are not suitable to be delivered directly to the zone due to their unacceptable effects on comfort requirements. In addition, the heating coil adds sensible heat to the zone while off-setting the variation in temperature.

2-3-4 Ventilation

The heat transfers by ventilation produces the temperature T_z and humidity ratio W_z of the zone, wherein the supply air and the zone conditions mix until reaching **point 4**. The conditioned air or supply air at **point 3** has a temperature T_{sa} equal to temperature of the air after the heating coil T_{hc}. At **point 3** the supply humidity ratio W_{sa} is equal to the heating coil humidity ratio W_{hc}, which is also equal to the humidity ratio of the air at the outlet of the cooling coil W_{cc}.

In addition, ventilation transports the air throughout all the ducting system, the coils and the zone (described by the circulation cycle **oa,4 - 1 - 2 - 4** in Figure 2-4). In which, some key aspects are the sensible and latent heat transfers from the supply air to the zone by the air mass flow rate, which contribute to an increases or decreases in the zone temperature and humidity ratio.

Fan power

The calculation of the power of the supply fan P_f is approximately proportional to the cube of the total supply airflow as shown below [12, 26, 27]:

$$P_f = \alpha_f \dot{m}_a^3 : \tag{2-3}$$

where $\dot{m}_a$ is the air mass flow rate expressed in [kgs^{-1}] and α_f=0.5 [kW s^{3}kg^{-3}] is the fan power constant, [26].

Fan Energy

The total energy consumption of the fan is given by:

$$E_{f,total} = \int_{t_{initial}}^{t_{final}} P_f dt \tag{2-4}$$

2-3-5 Heat calculation

The analyses of the previous processes are quantified by its enthalpy or total heat transfers. In Figure 2-4, the enthalpy of the cooling and dehumidification processes is equal to the heat injected by the cooling and the heating coils to the system. This statement is supported by the energy balance and thermodynamics laws. Also, the psychrometric chart clearly shows the relationship among the vectors describing the enthalpy across the coils.

Enthalpy

The vector enthalpy h_t corresponds to the difference from **point 3** to **point 1**, and it sums up the enthalpy vector of the cooling coil h_{cc} and the enthalpy of the heating coil vector h_{hc}.

The enthalpy of the cooling coil h_{cc} corresponds to the difference between **point 1** and **point 2**, which is expressed as:

$$h_{\mathrm{cc}} = c_{\mathrm{a}}(T_{\mathrm{cc}} - T_{\mathrm{ma}}) + h_{\mathrm{wv}}(W_{\mathrm{sa}} - W_{\mathrm{ma}}) \tag{2-5}$$

The enthalpy of the heating coil h_{cc} corresponds to the difference between **point 2** and **point 3**, which can be expressed as sensible heat:

$$h_{\mathrm{hc}} = c_{\mathrm{a}}(T_{\mathrm{sa}} - T_{\mathrm{cc}}) \tag{2-6}$$

The enthalpy of the system h_{t} then follows:

$$h_{\mathrm{t}} = h_{\mathrm{hc}} + h_{\mathrm{cc}} \tag{2-7a}$$
$$h_{\mathrm{t}} = c_{\mathrm{a}}(T_{\mathrm{sa}} - T_{\mathrm{ma}}) + h_{\mathrm{wv}}(W_{\mathrm{sa}} - W_{\mathrm{ma}}) \tag{2-7b}$$

Heat transfer rate

Using the developments from (2-5), (2-6) and (2-7), we can compute the heat transfers across the cooling coil $\dot{Q}_{\mathrm{cc}}$, the heating coil $\dot{Q}_{\mathrm{hc}}$ and the total heat $\dot{Q}_{\mathrm{t}}$ as follows:

$$\dot{Q}_{\mathrm{cc}} = \dot{m}_{\mathrm{a}}\left(c_{\mathrm{a}}(T_{\mathrm{cc}} - T_{\mathrm{ma}}) + h_{\mathrm{wv}}(W_{\mathrm{sa}} - W_{\mathrm{ma}})\right) \tag{2-8a}$$
$$\dot{Q}_{\mathrm{hc}} = \dot{m}_{\mathrm{a}}\left(c_{\mathrm{a}}(T_{\mathrm{sa}} - T_{\mathrm{cc}})\right) \tag{2-8b}$$
$$\dot{Q}_{\mathrm{t}} = \dot{m}_{\mathrm{a}}\left(c_{\mathrm{a}}(T_{\mathrm{sa}} - T_{\mathrm{ma}}) + h_{\mathrm{wv}}(W_{\mathrm{sa}} - W_{\mathrm{ma}})\right) \tag{2-8c}$$

From the set of equations (2-8), (2-8c) can be used as a surrogate of the dynamics of the coils. As it will be shown in Chapter 3, we use the structure of the MPC algorithm to include (2-8c) in the cost function, in which we define $\dot{m}_{\mathrm{a}}$, T_{sa} and W_{sa} as decision variables.

Saturation equation

This equation represents the dry-bulb temperature to the humidity ratio when the relative humidity is 100%. We have previously declared the humidity ratio of the supply air as decision variables in the control problem. However, the controlled variable in the cooling coil is its off-coil air temperature; for the heating coil, the controlled variable is the temperature T_{sa}, which is equal to its off-coil air temperature. We proceed to obtain the off cooling coil air temperature T_{cc} by approximating the curve of the temperature as a function of the humidity ratio in the psychrometric chart at saturation. This approximation was chosen as a second order equation of the form:

$$T_{\mathrm{cc}} = aW_{\mathrm{sa}}^2 + bW_{\mathrm{sa}} + c \tag{2-9}$$

where a, b and c are constant parameters obtained by the nonlinear least-squares (nonlinear data-fitting) problem:

$$\min_x ||e(x)||_2^2 \tag{2-10}$$

$$\begin{aligned} x &= [a, b, c] \\ e(x) &= aW_{\text{fit}}^2 + bW_{\text{fit}} + c - T_{\text{fit}} \end{aligned}$$

where T_{fit} is the temperature vector of values in the interval $[-17, 100]$, and $W_{\text{fit}} = f(T_{\text{fit}})$ the computed humidity ratio obtained from (A-7) at saturation where the relative humidity is equal to 100%.

2-4 Modeling of the system dynamics

The system dynamics model corresponds to the analysis of the zone, where the states, inputs, and disturbances are described in Section 2-4-2. This simplification of the system from Figure 2-2 to the zone model reduces the complexity of the system and thus the controller synthesis. This choice was made since the dynamics of the coils correspond to a highly nonlinear discrete time MIMO system. Even though there was found in literature some efforts to model the coils as simplified representations as done in [28, 29], in regard to cooling coils, those models do not capture the processes of cooling and dehumidification. Moreover, those nonlinear representations lead to a hard problem to solve using MPC. In addition, while a system identification and filtering technique can be applied to find the parameters of the integrate model of the system, the availability of data is a determining factor. This data was not available for the development of this work, and neither system identification nor filtering techniques were considered as the core of this project.

Before introducing the mathematical model, the considerations and assumptions are presented next.

2-4-1 Assumptions

- The HVAC system from Figure 2-2 is oversimplified, which means that the heating and cooling coils dynamics are neglected. This is accomplished by considering the conditioned air temperature T_{sa} and humidity ratio W_{sa} as controlled inputs. These inputs are controlled in the air conditioning units, where W_{sa} is the controlled variable of the cooling coil and T_{sa} is the surrogate for sensible heating or cooling by the coils.
- The building is assumed to be a single zone space, which is represented by one temperature T_{z} and humidity ratio W_{z}. These variables represent an average value of the whole space. While the relative humidity in the zone RH_{z} is not considered here, its quantification is a consequence of the temperature T_{z} and humidity ratio W_{z}, (A-8).
- The humidity ratio W_{z} in the building is assumed to be only affected by occupancy, thus, other sources of moisture are neglected, such as infiltration from the outside weather conditions, moisture from built-in materials of the construction, or building defects (piping leaks, rain penetration, envelope cracks).

- The air is considered to have an ideal gas behavior, perfect mixing, constant pressure, and during its conditioning processes the thermal losses are negligible. Moreover, the air specific heat capacities and densities are considered to be constant parameters.

2-4-2 Mathematical equations

The model follows the governing generalized equations of the heat transfer and preservation of energy and mass given by:

$$C\frac{dT}{dt} = \dot{Q} \tag{2-11a}$$

$$M\frac{dW}{dt} = \dot{W} \tag{2-11b}$$

where C and M are the thermal capacity and mass of the air in certain space, $\frac{dT}{dt}$ is the temperature variation, $\frac{dW}{dt}$ is the humidity ratio variation and $\dot{Q}$ and $\dot{W}$ accounts for the sum of the sensible and latent heat transfers, respectively.

We define the states, inputs and disturbances of the model of the zone as following:

States

- T_{z}, Temperature of air inside the zone
- W_{z}, Humidity ratio of the air inside the zone

Control inputs

- $\dot{m}_{\mathrm{a}}$, Mass flow rate of the air
- T_{sa}, Temperature of the supply air
- W_{sa}, Humidity ratio of the supply air

Disturbances

- T_{oa}, Temperature outside air
- I_{o}, Solar radiation
- $\dot{Q}_{\mathrm{int}}$, Sensible heat transfers sum from internal sources of the zone
- $\dot{W}_{\mathrm{int}}$, Latent heat transfers sum from internal sources of the zone

Parameters

- ρ_{a}, Density of air
- c_{a}, Specific heat capacity of air
- h_{wv}, Specific enthalpy of water vapor
- C_{z}, Thermal capacitance of the zone
- M_{z}, Moisture capacitance on the zone
- A_{win}, A_{wall} and A_{floor}, Area of windows, walls and floor
- SGF, Solar gain factor
- U_{wall}, Thermal transmittance of the wall
- cf_{win}, cf_{per}, cf_{eq} and cf_{light} , Convection factor of windows, persons, equipment and lighting
- ϵ_{per}, ϵ_{eq}, and $\epsilon_{\mathrm{light}}$, emissivity factor of persons, equipment and lighting
- q_{eq} and q_{light}, Heat flux of equipment and lighting
- C_{per}, Heat per person
- H_{per}, Moisture rate per person

Zone temperature dynamics

Following the first law of thermodynamics (energy conservation), the temperature evolution of the zone T_{z} is given as:

$$C_{\mathrm{z}}\frac{dT_{\mathrm{z}}}{dt} = \rho_{\mathrm{a}}c_{\mathrm{a}}\dot{m}_{\mathrm{a}}(T_{\mathrm{sa}} - T_{\mathrm{z}}) + \dot{Q}_{\mathrm{int}} \tag{2-12}$$

where the first term from the right hand side corresponds to the heat transfer between the AHU ventilation system and the zone. Here, T_{sa} is the temperature of the supplied air, which is the temperature of the air that has been conditioned by the cooling and heating coils. The second term $\dot{Q}_{\mathrm{int}}$ corresponds to the internal sensible heat loads, which follows, [30]:

$$\dot{Q}_{\mathrm{int}} = \dot{Q}_{\mathrm{env}} + \dot{Q}_{\mathrm{people}} + \dot{Q}_{\mathrm{inst}} \tag{2-13}$$

where $\dot{Q}_{\mathrm{env}}$ is the sensible heat produced by the environment, namely outside temperature and solar radiation, $\dot{Q}_{\mathrm{people}}$ is the heat from people, $\dot{Q}_{\mathrm{eq}}$ is the heat from equipment and lighting. The former can be computed from:

$$\dot{Q}_{\mathrm{env}} = U_{\mathrm{wall}}A_{\mathrm{wall}}(T_{\mathrm{oa}} - T_{\mathrm{z}}) + SGFA_{\mathrm{win}}I_{\mathrm{o}}cf_{\mathrm{win}} \tag{2-14}$$

where the first term corresponds to the heat gain due to the difference between the outside temperature T_{oa} and the zone temperature T_{z}. In this first term, A_{wall} is the area of the

wall and U_{wall} the wall thermal transmittance. The second term is the heat gain due to solar radiation. From (2-13), $\dot{Q}_{\text{people}}$ follows:

$$\dot{Q}_{\text{people}} = cf_{\text{per}} C_{\text{per}} N_{\text{per}} \tag{2-15}$$

where the right hand side represents the heat gain of people resulting from their short wave radiative heat contribution into the zone.

From (2-13), the heat from installation is $\dot{Q}_{\text{ins}} = \dot{Q}_{\text{eq}} + \dot{Q}_{\text{light}}$, in which:

$$\dot{Q}_{\text{eq}} = cf_{\text{eq}} A_{\text{floor}} q_{\text{eq}}, \tag{2-16}$$

expression that represents the short wave radiation produced by the heat transfer from installations. Similarly, the heat gain from lighting is:

$$\dot{Q}_{\text{light}} = cf_{\text{light}} A_{\text{floor}} q_{\text{light}} \tag{2-17}$$

The factors cf_{per}, cf_{eq} and cf_{light} in (2-15), (2-16) and (2-17) are computed from:

$$cf_{\text{per}} = 1 - \epsilon_{\text{per}} \tag{2-18a}$$
$$cf_{\text{eq}} = 1 - \epsilon_{\text{eq}} \tag{2-18b}$$
$$cf_{\text{light}} = 1 - \epsilon_{\text{light}} \tag{2-18c}$$

where ϵ_{per}, ϵ_{eq} and ϵ_{light} are the emissivity factors of each surface, namely people skin, installations surfaces and lighting surfaces.

Considering the heat gain of walls from (2-14) as an independent heat gain, since it relates to the zone temperature T_{z}, the dynamics of the temperature T_{z} in a compact representation are given as:

$$C_{\text{z}} \frac{dT_{\text{z}}}{dt} = c_{\text{a}} \dot{m}_{\text{a}} (T_{\text{sa}} - T_{\text{z}}) + U_{\text{wall}} A_{\text{wall}} \dot{m}_{\text{a}} (T_{\text{oa}} - T_{\text{z}}) + \dot{Q}_{\text{int}} \tag{2-19}$$

$$\frac{dT_{\text{z}}}{dt} = k_{1\text{z}} \dot{m}_{\text{a}} (T_{\text{sa}} - T_{\text{z}}) + k_{2,\text{z}} \dot{m}_{\text{a}} (T_{\text{oa}} - T_{\text{z}}) + k_{3,\text{z}} \dot{Q}^1_{\text{int}} \tag{2-20}$$

where

$$k_{1,\text{z}} = \frac{c_{\text{a}}}{C_{\text{z}}}, k_{2,\text{z}} = \frac{U_{\text{wall}} A_{\text{wall}}}{C_{\text{z}}}, k_{3,\text{z}} = \frac{1}{C_{\text{z}}}$$

and $\dot{Q}^1_{\text{int}} = \dot{Q}_{\text{solar}} + \dot{Q}_{\text{people}} + \dot{Q}_{\text{inst}}$.

Zone Humidity ratio dynamics

Following the mass conservation principles, the dynamics of the humidity ratio W_{z} in the zone are given as:

$$M_{\text{z}} \frac{dW_{\text{z}}}{dt} = \dot{m}_{\text{a}} (W_{\text{sa}} - W_{\text{z}}) + \dot{W}_{\text{int}} \tag{2-21}$$

where the first term of the right hand side corresponds to the humidity variation due to the AHU humidity ratio W_{sa} in response to the zone humidity ratio W_{z}, and the second term is

the addition of moisture due to the latent loads in the zone, $\dot{W}_{\text{int}}$, which will be assumed to be caused by occupancy:

$$\dot{W}_{\text{int}} = N_{\text{per}} H_{\text{per}} \tag{2-22}$$

where, H_{per} is the moisture rate per person. Then, the dynamics of the humidity ratio W_{z} in a compact representation are:

$$\frac{dW_{\text{z}}}{dt} = k_{4,\text{z}} \dot{m}_{\text{a}} (W_{\text{sa}} - W_{\text{z}}) + k_{4,\text{z}} \dot{W}_{\text{int}} \tag{2-23}$$

where,

$$k_{4,\text{z}} = \frac{1}{M_{\text{z}}}$$

Summary of equations

Define the state vector $[x_1, x_2]^\top = [T_{\text{z}}, W_{\text{z}}]^\top$, as the temperature and humidity ratio of the zone, the control inputs $[u_1, u_2, u_3]^\top = [m_{\text{sa}}, T_{\text{sa}}, W_{\text{sa}}]^\top$ as the mass flow, the temperature and the humidity ratio of the supply air and the disturbances as $[d_1, d_2, d_3]^\top = [T_{\text{oa}}, \dot{Q}_{\text{int}}, \dot{W}_{\text{int}}]^\top$ as the temperature of the outside air, internal heat gains, and latent gains, the compact representation of (2-20) and (2-23) follows:

$$\frac{dx_1}{dt} = k_{1,\text{z}} u_1 (u_2 - x_1) + k_{2,\text{z}} (d_1 - x_1) + k_{3,\text{z}} d_2 \tag{2-24a}$$

$$\frac{dx_2}{dt} = k_{4,\text{z}} u_1 (u_3 - x_2) + k_{4,\text{z}} d_3 \tag{2-24b}$$

where,

$$k_{1,\text{z}} = \frac{c_{\text{a}}}{C_{\text{z}}}, k_{2,\text{z}} = \frac{U_{\text{wall}} A_{\text{wall}}}{C_{\text{z}}}, k_{3,\text{z}} = \frac{1}{C_{\text{z}}}, k_{4,\text{z}} = \frac{1}{M_{\text{z}}}$$

The system (2-24) represents a nonlinear continuous time MIMO system of the temperature and humidity ratio of the zone. Here the input u_1 has a polynomial relation with respect to u_2 and u_3, and a bilinear relation with the states x_1 and x_2.

Chapter 3

Controller design

The focus of this chapter is the design of the Model Predictive Control (MPC) of the system shown in Figure 3-2. In Section 3-1, we introduce the discretization of the model followed by Section 3-2, in which the objectives of the control strategy are described. Section 3-3 presents the MPC, the assumptions made and the controller design. The MPC problem formulation is presented in Section 3-4. We conclude this chapter with a numerical example in Section 3-5.

3-1 Discretization and sampling time selection

The Euler forward method was used to develop the discrete-time system of the continuous time system from (2-24). The approximation of $\dot{x}$ is given as:

$$\dot{x} = \frac{x_{k+1} - x_k}{\Delta T}$$

Here, the knowledge of x_k, the time step or sampling time ΔT, and the derivative $\dot{x}$ are used to approximate the slope between the current and the next point x_{k+1}. This algorithm is known as an *explicit* integration method since it uses past and current values. Figure 3-1 illustrates where the current value of x at time t is used to approximate the slope, [5].

Forward discretization showed numerical stability for the case of study described in Section 3-5. However, to guarantee unconditional stability backward discretization is preferable. This approach is a well suited method for building discrete time systems with low sampling rates, as proved in [31].

The sampling time chosen was $\Delta T = 15$ minutes, a period sufficiently enough to capture the system dynamics [32]. The continuous system from (2-24) is then expressed as the discrete-time nonlinear system, which yields to:

$$x_{1,k+1} = x_{1,k} + \Delta T \left(k_{1,z} u_{1,k}(u_{2,k} - x_{1,k}) + k_{2,z}(d_{1,k} - x_{1,k}) + k_{3,z} d_{2,k}\right) \tag{3-1a}$$

$$x_{2,k+1} = x_{2,k} + \Delta T (k_{4,z} u_{1,k}(u_{3,k} - x_{2,K}) + k_{4,z} d_{3,k}) \tag{3-1b}$$

$$y_k = C x_k \tag{3-1c}$$

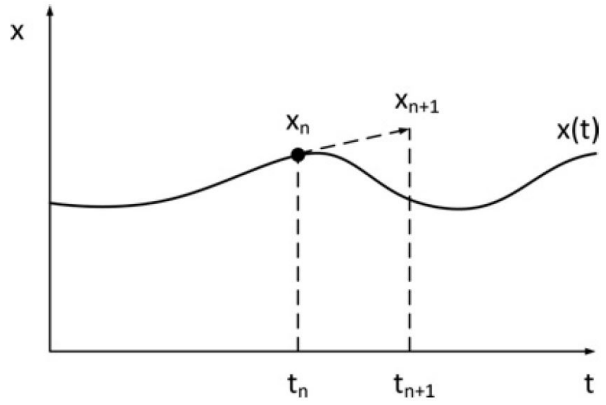

Figure 3-1: Representation of the Euler forward method, [5]

The aforementioned developments can be rewritten as a single dynamical model for each sampling time k in a more compact notation:

$$x_{k+1} = f(x_k, u_k, d_k) \tag{3-2a}$$
$$y_k = h(x_k, u_k, d_k) \tag{3-2b}$$

where the discrete state vector is $x_k := [x_{1,k}, x_{2,k}]^\top = [T_\mathrm{z}, W_\mathrm{z}]^\top \in \mathbb{R}^2$, the output vector is $y_k := x_k \in \mathbb{R}^2$, the vector of inputs is $u_k := [u_{1,k}, u_{2,k}, u_{3,k}]^\top = [m_{\mathrm{a},k}, T_{\mathrm{sa},k}, W_{\mathrm{sa},k}]^\top \in \mathbb{R}^3$ and the vector of disturbances $d_k := [d_{1,k}, d_{2,k}, d_{3,k}]^\top = [T_{\mathrm{oa},k}, \dot{Q}_{\mathrm{int},k}, \dot{W}_{\mathrm{int},k}]^\top \in \mathbb{R}^3$, where $\dot{Q}_{\mathrm{int},k} = f(\dot{Q}_{\mathrm{solar}}, \dot{Q}_{\mathrm{people}}, \dot{Q}_{\mathrm{ins}})$ and $\dot{W}_{\mathrm{int},k} = f(\dot{W}_{\mathrm{people}})$.

3-2 Objectives of the control strategy

As described in the previous chapters, the main goal is to obtain an energy efficient system while guaranteeing comfort conditions in temperature and humidity. Thus, the control objectives are straightforwardly described as follows:

- The temperature T_z, humidity ratio W_z and relative humidity RH_z inside the zone are kept under comfort conditions. Here, we define comfort conditions to be fixed values of temperature and humidity:

$$T_{\mathrm{z,sp}} = 20\ [^\circ\mathrm{C}] \tag{3-3a}$$
$$W_{\mathrm{z,sp}} = 8\ [\mathrm{g_w kg_a^{-1}}] \tag{3-3b}$$
$$RH_{\mathrm{z,sp}} = 55.62\ [\%] \tag{3-3c}$$

- The energy used by the cooling and heating coils is minimized, which consequently means a reduction in the costs associated to the production units.

- The constraints of the temperatures and humidity ratios of the zone and supply air are satisfied.

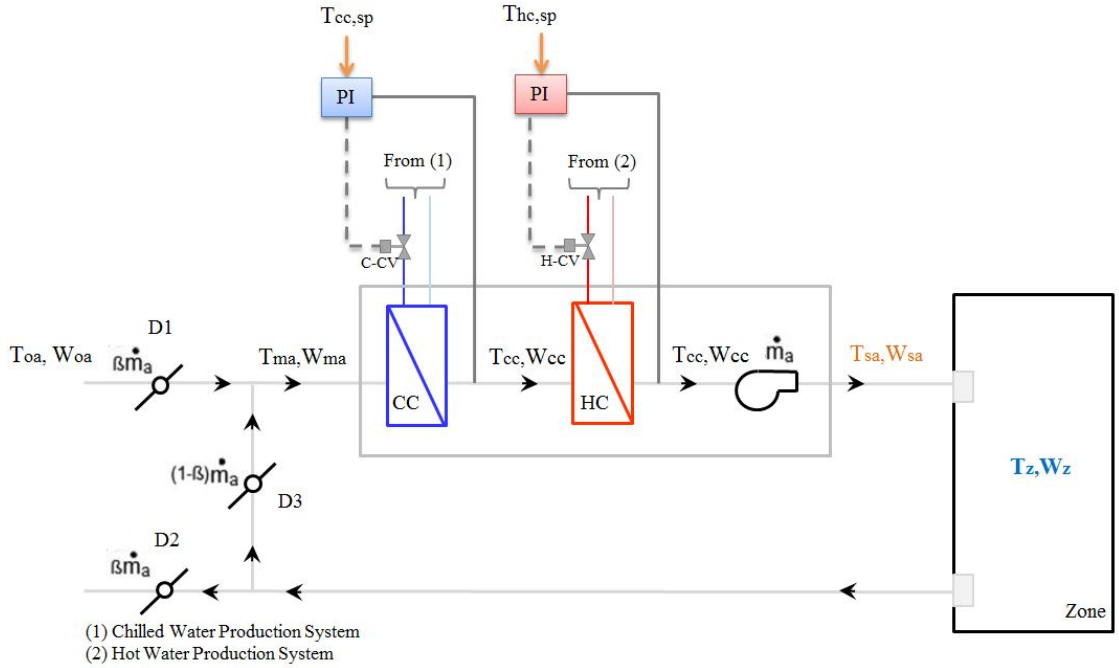

Figure 3-2: HVAC control system

3-3 Model Predictive Control

It is an algorithm that optimizes the control signal using the prediction of the evolution of system by means of its dynamical model and the constraints imposed. It uses the explicit knowledge of the dynamical model and allows the quantification of the control objectives in the cost function while keeping the states and inputs within bounds, see a more detailed explanation in Appendix B.

The optimization problem of our system aims to minimize the control objectives described in Section 3-2 by computing the optimal air conditioning input trajectories over the control horizon while keeping the temperatures, humidity ratios and inputs within bounds. These optimal control input trajectories result in trajectories for temperature and humidity ratio of the zone. Only the first input is applied to the system. Then, measurements are performed to estimate the next state. Subsequently, the optimal control computation is repeated over the new time horizon starting from the next estimated state.

3-3-1 Motivation

For temperature and humidity control in buildings, MPC presents a series of advantages in comparison to classic control methods. It stands out the intuitive concepts that relate temperature and humidity to energy consumption, relation which in PID or rule-based methods is not straightforward. Also, the treatment of constraints in temperature and humidity ratio of the zone and inputs is conceptually simple and can be systematically included during the design process. Moreover, MPC is a well adopted method for processes with slow dynamics, which is the case of our system. A major shortcoming of MPC is the need of an appropriate

model of the process to be available, thus, discrepancies between the real process and the model used will affect the results of the controller.

3-3-2 Tuning parameters

Prediction horizon, N_p

It represents the length of the finite horizon open-loop optimal control problem solved at each time step. A higher value of N_p captures the dynamics up to the permanent regime, and increases the domain of attraction of the controller and performance. However, the length of the predictions increases as well as the number of decision variables hence the complexity of the optimization problem, [8].

Considering the state representation of the nonlinear system (3-1), the availability of full state information and predictions at each sampling time, we defined a prediction N_p horizon of 20 time steps, which is equivalent to 5 hours in time. Hence, at each time step the prediction data of the next 5 hours is also incorporated in the optimization problem.

Control horizon, N_c

This parameter corresponds to number of time steps over which the optimal control input trajectories are computed at each time step, [8].

To allow flexibility in the control action and avoid aggressive control actions, we kept the control horizon N_c equal to the prediction horizon $N_p = 20$.

3-3-3 Assumptions

The design of the nonlinear MPC is based on the statements from Section 2-4-1 and the following assumptions and considerations:

- The relative humidity RH_z is indirectly controlled by limiting the temperature T_z and humidity ratio W_z within bounds. We defined the limits by a region in the psychrometric chart around the set-points in temperature $T_{z,sp}$ and humidity ratio $W_{z,sp}$, as shown in (3-3-5).
- Low-level controllers control the water flow rates of the chilled $(C - CV)$ and hot water $(H - CV)$ valves of the cooling and heating coils, respectively. It is assumed these controllers track the set-points $T_{cc,sp} = f(W_{sa})$, which is computed by (2-9), and $T_{hc} = T_{sa}$. The design and implementation of these low-level controllers are not part of this thesis.
- W_{sa} and T_{sa} are considered as decision variables for the nonlinear MPC. These inputs together with the air flow rate input $\dot{m}_a$ are within the capacity of the coils and fan, which means that the HVAC system in the air side is properly sized. Thus, the water side or production units are capable to deliver enough heat from the water to produce those inputs.

- The dampers opening are not a controlled inputs. It is assumed 20% of fresh air from the outside is drawn into the system, which guarantees air quality. Then, the mixed air conditions satisfy the formula (2-2).
- The predictions of the disturbances from the weather conditions, sensible and latent heat gains of the zone are assumed to be available for the simulation time.

3-3-4 Cost function

The objective of the MPC controller is to obtain a comfortable indoor temperature T_{z} and humidity ratio W_{z} with the least energy consumption. Our goal is to find the inputs $u_1 = \dot{m}_{\mathrm{a}}, u_2 = T_{\mathrm{sa}}$ and $u_3 = W_{\mathrm{sa}}$ at each sampling time k. The cost function J_k is then associated to the reference tracking problem ($J_{1,k}$, $\mathrm{J}_{2,k}$), which ensures the comfort conditions, and the energy consumption problem(J_3):

$$J = J_{1,k} + J_{2,k} + J_{3,k} \tag{3-4}$$

where,

- $J_{1,k} = \|y_{1,k} - T_{\mathrm{sp}}\|^2_{Q_{\mathrm{T}}}$, penalizes the deviation of the room temperature from its set-point T_{sp} by the weighting factor Q_{T}
- $J_{2,k} = \|y_{2,k} - W_{\mathrm{sp}}\|^2_{Q_{\mathrm{W}}}$, penalizes the deviation of the room humidity ratio from its set-point W_{sp} by the weighting factor Q_{W}.
- $J_{3,k} = ||u_1||^2_{Q_u} + F_k$, corresponds to the energy related term. Herein, F_k corresponds to one of the scenarios presented next, which are analyzed in terms the air mass flow rate F_1, the sensible heat F_2 from ventilation, and enthalpy F_3.

Air mass flow rate

This function corresponds to the optimization with respect to the air mass flow rate $\dot{m}_{\mathrm{a}} = u_1$. This input affects the heat transfer across both coils, see the general equation of heat (2-8). Here, $F_1 = 0$, and J_3 yields to:

$$J_{3,k} \quad = \quad ||u_1||^2_{Q_{\mathrm{u}}} \tag{3-5}$$

In (3-5), Q_{u} corresponds to the air mass flow rate weighting factor. This cost was chosen since the heat of the coils can be expressed as:

$$\dot{Q} = c_{\mathrm{a}} \dot{m}_{\mathrm{a}} \Delta T, \tag{3-6}$$

where c_{a} is the specific heat capacity of the air, $\dot{m}_{\mathrm{a}}$ the air mass flow rate and ΔT the difference between the off- and in- coil temperatures. Even though the dynamics of the coils have not been modelled, it is possible to compute the temperature of the coils from the solution u of the MPC and the energy and mass conservation laws. The relation of $u_1 = \dot{m}_{\mathrm{a}}$ in (3-36) allows us to have an indirect control of the heat rate of the coils and it also optimizes the fan power consumption.

Sensible heat

(3-7) was chosen due to the findings from literature, in which it was considered that the heat from ventilation $\dot{Q}_{\text{vent}} = c_{\text{a}}\dot{m}(T_{\text{sa}} - T_{\text{z}})$ corresponded to the total heat provided by a coil. The psychrometric analysis from Section 2-3 showed that this does not hold. F_2 is expressed as:

$$F_2 = \dot{Q}_{\text{vent}} = \tau \dot{m}_{\text{a}} c_{\text{a}} (T_{\text{sa}} - T_{\text{z}}) \tag{3-7}$$

In this equation, τ is a constant weight, $\dot{m}_{\text{a}} = u_1$ the air mass flow rate, c_{a} the heat capacity of the air, $T_{\text{sa}} = u_2$ the temperature of the supply air and $T_{\text{z}} = x_1$ the temperature of the zone. Then, J_3 follows:

$$J_{3,k} = ||u_1||^2_{Q_u} + \tau c_{\text{a}} u_1 |u_2 - x_1| \tag{3-8}$$

Enthalpy

(3-9) allows us to optimize the heat load of the cooling and heating coils. This function is assessed by the psychrometric analysis of the moist air throughout the HVAC system, see Section 2-3. In this cost, the dynamics of the coils are not required. Moreover, the constant value for β introduces T_{ma} and W_{ma} as variables that can be computed from (2-2). Then, F_3 is expressed as:

$$F_3 = \tau \dot{m}_{\text{a}} \left(c_{\text{a}} T_{\text{sa}} + h_{\text{wv}} W_{\text{sa}} - (c_{\text{a}} T_{\text{ma}} + h_{\text{wv}} W_{\text{ma}}) \right), \tag{3-9}$$

where, τ is a constant weight, $\dot{m}_{\text{a}} = u_1$ the air mass flow rate, c_{a} the heat capacity of the air, h_{wv} the specific heat capacity of the water vapor, $T_{\text{sa}} = u_2$ the temperature of the supply air, T_{ma} the temperature of the mixed air, W_{sa} the humidity ratio of the supply air, and W_{ma} the humidity ratio of the mixed air. The energy cost term J_3 is given as:

$$J_{3,k} = ||u_1||^2_{Q_u} + \tau u_1 \left| c_{\text{a}} u_2 + h_{\text{wv}} u_3 - (c_{\text{a}} T_{\text{ma}} + h_{\text{wv}} W_{\text{ma}}) \right| \tag{3-10}$$

3-3-5 Constraints

The limits of the sets $\mathcal{X}$, $\mathcal{Y}$ and $\mathcal{U}$ from Section 3-4 are presented in this section. Here the state set $\mathcal{X}$ is equal to the output set $\mathcal{Y}$.

Comfort

The building (zone) temperature and humidity ratio, which correspond to the system states x_k, have to be kept in a range that complies with thermal comfort. We consider such limits as the set $\mathcal{X}$ between the following values:

$$\underline{T_{\text{z}}} \leq x_{1,k} \leq \overline{T_{\text{z}}} \tag{3-11a}$$
$$\underline{W_{\text{z}}} \leq x_{2,k} \leq \overline{W_{\text{z}}} \tag{3-11b}$$

where $\underline{T_z}$, $\overline{T_z}$, $\underline{W_z}$ and $\overline{W_z}$ are chosen so that the relative humidity RH is kept between 40% and 60%. Considering $x_{sp} = [T_{sp}, W_{sp}]^\top$, where $T_{sp} = 20$ [°C] and , $W_{sp} = 8$ [$g_w kg_a^{-1}$], the chosen limits are:

$$\underline{T_z} = 18\ [°C] \quad \text{and} \quad \overline{T_z} = 21\ [°C] \tag{3-12a}$$

$$\underline{W_z} = 6\ [g_w kg_a^{-1}] \quad \text{and} \quad \overline{W_z} = 8,3\ [g_w kg_a^{-1}] \tag{3-12b}$$

Although the nonlinear function of the relative humidity $RH_z = f(Tz, W_z)$ computed from (A-9) is not included in the system dynamics, by including the reference tracking of the states to x_{sp} in the cost function (3-4) and the state constraints (3-12), the relative humidity in the zone RH_z remains in the psychrometric region around the point x_{sp}.

Supply air inputs

These constraints correspond to the air mass flow rate of the fan and to the heating and cooling coil capacities, which describes the set $\mathcal{U}$.

The air mass flow rate limits are given by:

$$\underline{m_{sa}} \leq u_{1,k} \leq \overline{m_{sa}} \tag{3-13}$$

where $\underline{m_{sa}} = 0.001$ [kgs^{-1}] is the lower limit considered to be different from zero since it is a common practice to deliver air into the building. The upper limit value is considered with regard to the number of air cycles $a_{A/C}$ desired within an hour to remove the air mass in the building volume. This limit was chosen equal to 8 (value considered according to a zone with considerable amount of people). Then, the air mass flow rate is computed as shown below.

$$\dot{m}_{calc} = V_z \rho_a a_{A/C} = 600 * \frac{8}{3600} = 1.3\ [kgs^{-1}] \tag{3-14}$$

where V_z is the volume of the zone, $a_{A/C}$ the air cycles per hour and ρ_a the density of the air. For this analysis, $\dot{m}_{calc} = 1.3$ is approximated to the upper integer value, value that corresponds to the upper air mass flow rate limit $\overline{m_{sa}} = 2$ [kgs^{-1}].

The conditioned air temperature T_{sa} corresponds to the surrogate of the temperature that can be obtained from the cooling and heating coils. It is related to the temperature after the cooling coils in the range:

$$\underline{T_{sa}} \leq u_{2,k} \leq \overline{T_{sa}} \tag{3-15}$$

where $\underline{T_{sa}}$ and $\overline{T_{sa}}$ correspond to the minimum and maximum temperatures that can be obtained by either the cooling coil or heating coil acting alone or in combination. Thus, the following values are admissible:

$$\underline{T_{sa}} = 12\ [°C] \quad \text{and} \quad \overline{T_{sa}} = 24\ [°C] \tag{3-16}$$

The conditioned air humidity ratio W_{sa} expresses the capacity of the cooling coil in terms of the amount of condensation that it can produce. This variable is related to the cooling coil and not the heating coil, and its limits are:

$$\underline{W_{\text{sa}}} \leq u_{3,k} \leq \overline{W_{\text{sa}}} \tag{3-17}$$

where $\underline{W_{\text{sa}}}$ is the minimum humidity ratio that can be produced by condensation as a result of the heat exchange between the chilled water production units and the air. It means that the chilled water can reach the temperature corresponding to the humidity ratio W_{sa}. $\overline{W_{\text{sa}}}$ is the maximum humidity ratio limit of the supply air. It is chosen as the mixed air humidity ratio W_{ma}, since it corresponds to the conditions that may be delivered to the zone. While it was not considered a humidification element, the humidity ratio of the supply air W_{sa} may behave as an increasing or decreasing source of moisture in the zone. The minimum and maximum values of the supply air humidity ratio are then assumed to have the following values:

$$\underline{W_{\text{sa}}} = 6\ [\text{g}_{\text{w}}\text{kg}_{\text{a}}^{-1}] \quad \text{and} \quad \overline{W_{\text{sa}}} = W_{\text{ma}} \tag{3-18}$$

3-3-6 Feasibility

The region of the sets in $\mathcal{X}$, $\mathcal{Y}$ and $\mathcal{U}$ defined earlier may not guarantee that the optimization algorithm finds a solution. The unfeasibility of the problem may be caused by the physical characteristics of the equipment for instance the maximum allowable fan velocity and the heating and cooling capacities of the coil expressed as the temperature T_{sa} and humidity ratio W_{sa} of the supply air. Another factor influencing feasibility is the transitory regime, where there exists incompatibility between the constraints with respect to the disturbances.

To recover feasibility we will relax the system by using soft constraints. The input constraints will not be relaxed since they correspond to physical characteristics thus the set $\mathcal{U}$ cannot be violated and will remain unchanged. The state constraints however are softened by the introduction of non negative slack variables as shown below:

$$\underline{x_{\text{z}}} - \begin{bmatrix}1\\1\end{bmatrix}\epsilon_2 \leq x \leq \overline{x_{\text{z}}} + \begin{bmatrix}1\\1\end{bmatrix}\epsilon_1 \quad \epsilon_1, \epsilon_2 \geq 0, x \in \mathcal{X}_{\text{c}} \tag{3-19}$$

were $x = [T_{\text{z}}, W_{\text{z}}]^\top$, $\underline{x_{\text{z}}} = [\underline{T_{\text{z}}}, \underline{W_{\text{z}}}]^\top$, $\overline{x_{\text{z}}} = [\overline{T_{\text{z}}}, \overline{W_{\text{z}}}]^\top$, and ϵ_1 and ϵ_2 are the non negative slack variables. These slack variables will allow the violation of the states constraints, from which the level of violation is defined as an additional linear cost J_ϵ that will be included in the objective function J from the equation (3-4).

$$J_\epsilon = \rho_1\epsilon_1 + \rho_2\epsilon_2 \tag{3-20}$$

Equation (3-20) represents the cost associated to the soft constraints of the states x, where the penalty weights ρ_1 and ρ_2 ensures the feasibility of the optimization problem. These weights must guarantee we have 'exact soft constraints' that enforces the hard constraints when the problem is feasible, [33]. Also, the tuning of ρ_1 and ρ_2 should avoid numerical issues and be greater than the infinity norm of the vector of Lagrange multipliers of the original problem, [34].

3-4 MPC problem formulation

Consider the cost function from 3-3-4, the input constraints 3-3-5, the soft constraints and penalty function from 3-3-6, the time step $k \in [0, 1, 2, \cdots N_\mathrm{p}]$, where N_p is the length of the prediction horizon, the state vector sequence $\boldsymbol{x} := [x(k)^\top \cdots x(N_\mathrm{p})^\top]$, and the input vector sequence $\boldsymbol{u} := [u(k)^\top \cdots u(N_\mathrm{p}-1)^\top]$. We can formulate a finite-horizon optimal control problem for each time step k as given as:

$$\begin{aligned}
\min_{\boldsymbol{u}} \quad & \sum_{k=0}^{N_\mathrm{p}} J(\boldsymbol{x}, \boldsymbol{u}) && \text{(3-21a)}\\
\text{s.t.} \quad & x_{k+1} = f(x_k, u_k, d_k),\ \ x_k \in \mathcal{X}_\mathrm{c} \subseteq \mathbb{R}^2 && \text{(3-21b)}\\
& y_k = h(x_k, u_k, d_k),\ \ y_k \in \mathcal{Y}_\mathrm{c} \subseteq \mathbb{R}^2 && \text{(3-21c)}\\
& u_k \in \mathcal{U} \subseteq \mathbb{R}^3 && \text{(3-21d)}
\end{aligned}$$

Replacing the system dynamics (3-1), the constraints (3-13), (3-15), (3-17), (3-19), and the penalty function of the soft constraints (3-20), the control problem is then expressed as:

$$\begin{aligned}
\min_{\boldsymbol{u}} \quad & \sum_{k=0}^{N_\mathrm{p}} \left(J(\boldsymbol{x}, \boldsymbol{u}) + \sum_{i=1}^{2} \rho_i \epsilon_i \right) && \text{(3-22a)}\\
x_{1,k+1} &= x_{1,k} + \Delta T \left(k_{1,\mathrm{z}} u_{1,k} (u_{2,k} - x_{1,k}) + k_{2,\mathrm{z}} (d_{1,k} - x_{1,k}) + k_{3,\mathrm{z}} d_{2,k} \right), && \text{(3-22b)}\\
& \forall k = 0, 1, \cdots, N_\mathrm{p} - 1 &&\\
x_{2,k+1} &= x_{2,k} + \Delta T (k_{4,\mathrm{z}} u_{1,k} (u_{3,k} - x_{2,K}) + k_{4,\mathrm{z}} d_{3,k}),\ \forall k = 0, 1, \cdots, N_\mathrm{p} - 1 && \text{(3-22c)}\\
y_k &= C x_k,\ \forall k = 0, 1, \cdots, N_\mathrm{p} - 1 && \text{(3-22d)}\\
& \underline{x_\mathrm{z}} - \begin{bmatrix} 1 \\ 1 \end{bmatrix} \epsilon_2 \leq y_k \leq \overline{x_\mathrm{z}} + \begin{bmatrix} 1 \\ 1 \end{bmatrix} \epsilon_1,\ \forall k = 1, 2, \cdots, N_\mathrm{p} && \text{(3-22e)}\\
& \underline{m_\mathrm{sa}} \leq u_{1,k} \leq \overline{m_\mathrm{sa}},\ \forall k = 0, 1, \cdots, N_\mathrm{p} - 1 && \text{(3-22f)}\\
& \underline{T_\mathrm{sa}} \leq u_{2,k} \leq \overline{T_\mathrm{sa}},\ \forall k = 0, 1, \cdots, N_\mathrm{p} - 1 && \text{(3-22g)}\\
& \underline{W_\mathrm{sa}} \leq u_{3,k} \leq \overline{W_\mathrm{sa}},\ \forall k = 0, 1, \cdots, N_\mathrm{p} - 1 && \text{(3-22h)}\\
& \epsilon_1, \epsilon_2 \geq 0 && \text{(3-22i)}
\end{aligned}$$

Define x_{t0} as the initial state vector and a given vector of disturbances d_t at each sampling time t. It is assumed that the prediction vector $\boldsymbol{x}$ of the system dynamics (3-21b) is known given the initial state $x_0 = x_{t0}$. The proposed optimization problem (3-22) is a constrained nonlinear program for the polynomial and bilinear relation of the inputs and states in the system dynamics, (3-22b) and (3-22c). The algorithm is summarized in Table 3-1.

Temperature and humidity ratio of the coils

As a remainder of the notation, the subscript *cc* is associated to the cooling coil, *hc* to the heating coil, *sa* to the supply air and *ma* to the mixed air.

The solution of (3-22) provides the set-points for the cooling and heating coils low-level controllers. However, a post-processing procedure is followed to discriminate unnecessary air dehumidification and to compute the temperature and humidity ratios of the coils. In this procedure, we identify three processes that may occur as a consequence of $u_2 = T_{\text{sa}}$ and $u_3 = W_{\text{sa}}$. These processes are heating, cooling, and cooling and dehumidification.

Before describing the aforementioned processes, the mixed air temperature T_{ma} and its dew-point temperature $T_{\text{d,ma}}$ are computed:

$$T_{\text{ma}} = \beta T_{\text{oa}} + (1-\beta)x_1 \tag{3-23a}$$

$$T_{\text{d,ma}} = T_{\text{ma}} - \frac{100 - RH_{\text{ma}}}{5} \tag{3-23b}$$

We define $\Delta W = |W_{\text{sa}} - W_{\text{ma}}|$ $[\text{g}_{\text{w}}\text{kg}_{\text{a}}^{-1}]$, and set the condition $\Delta W \leq 1$. This band allows us to avoid dehumidifying the air in the inlet of the cooling coil for small changes in W_{sa}. Then, we proceed to compute the temperatures $T_{\text{cc}}, T_{\text{hc}}$ and humidity ratios $W_{\text{cc}}, W_{\text{hc}}$ of the coils in each of the following processes.

Heating: This process corresponds to the sensible heating of the air, which is a process that does not vary its humidity ratio. While avoiding unnecessary dehumidification, which is expressed as the deadband $\Delta W \leq 1$, heating occurs when the supply air temperature is greater than the mixed air and dew-point temperatures. These conditions are expressed as:

$$T_{\text{sa}} \geq T_{\text{ma}} \wedge T_{\text{sa}} > T_{\text{d,ma}} \wedge \Delta W \leq 1$$

Then, the air temperatures and humidity ratios of the coils are:

$$T_{\text{cc}} = T_{\text{ma}} \tag{3-24a}$$

$$W_{\text{cc}} = W_{\text{ma}} \tag{3-24b}$$

$$T_{\text{hc}} = T_{\text{sa}} \tag{3-24c}$$

$$W_{\text{sa}} = W_{\text{hc}} = W_{\text{ma}} \tag{3-24d}$$

Cooling: This process corresponds to sensible cooling, where no dehumidification is required, which is assumed as the dead band $\Delta W \leq 1$. Here, the supply air temperature is less than the mixed air temperature but greater than the dew-point temperature. These conditions are expressed as:

$$T_{\text{sa}} < T_{\text{ma}} \wedge T_{\text{sa}} > T_{\text{d,ma}} \wedge \Delta W \leq 1$$

The air temperatures and humidity ratios of the coils are:

$$T_{\text{cc}} = T_{\text{sa}} \tag{3-25a}$$

$$W_{\text{cc}} = W_{\text{ma}} \tag{3-25b}$$

$$T_{\text{hc}} = T_{\text{cc}} \tag{3-25c}$$

$$W_{\text{sa}} = W_{\text{hc}} = W_{\text{ma}} \tag{3-25d}$$

Cooling and dehumidification: This process corresponds to sensible and latent cooling, in which the deadband $\Delta W > 1$ determines the need for dehumidification. It also involves

the re-heating of the air after it has been dehumidified. Here, the supply air temperature is less than the mixed air and the dew-point temperatures. These conditions are expressed as:

$$T_{\mathrm{ma}} \wedge T_{\mathrm{sa}} \leq T_{\mathrm{d,ma}} \wedge \Delta W > 1$$

The temperatures and humidity ratios of the heating and cooling coils are given as:

$$\begin{aligned} T_{\mathrm{cc}} &= aW_{\mathrm{sa}}^2 + bW_{\mathrm{sa}} + c && \text{(3-26a)} \\ W_{\mathrm{cc}} &= W_{\mathrm{sa}} && \text{(3-26b)} \\ T_{\mathrm{hc}} &= T_{\mathrm{sa}} && \text{(3-26c)} \\ W_{\mathrm{sa}} = W_{\mathrm{hc}} &= W_{\mathrm{cc}} && \text{(3-26d)} \end{aligned}$$

Heat: (3-24), (3-25) and (3-26) allows us to compute the cooling and heating heat transfers $\dot{Q}_{\mathrm{cc}}, \dot{Q}_{\mathrm{hc}}$ which yields to:

$$\begin{aligned} \dot{Q}_{\mathrm{cc}} &= \dot{m}_{\mathrm{a}} \left(c_{\mathrm{a}}(T_{\mathrm{cc}} - T_{\mathrm{ma}}) + h_{\mathrm{wv}}(W_{\mathrm{sa}} - W_{\mathrm{ma}}) \right) && \text{(3-27a)} \\ \dot{Q}_{\mathrm{hc}} &= \dot{m}_{\mathrm{a}} c_{\mathrm{a}} (T_{\mathrm{hc}} - T_{\mathrm{cc}}) && \text{(3-27b)} \end{aligned}$$

Table 3-1: Algorithm Nonlinear MPC

Algorithm Nonlinear Model Predictive Control (MPC)	
1:	Initialize the state vector $x_0 = x_{\mathrm{t0}}$ and the disturbance vector along the prediction horizon $\{d\}_{k=0}^{N_{\mathrm{p}}}$.
2:	Solve the optimization program (3-21) and determine an optimal solution sequence $[u_0^*, \cdots, u_{N_{\mathrm{p}}}^*]$.
4:	Check if $u_{3,t0}^*$ triggers the dehumidification condition for small changes and compute the new $u_{3,t0}^{**}$, see Section 3-4.
3:	Apply the first element of optimal solution with $u_{3,t0}^* = u_{3,t0}^{**}$, which yields to input vector $u_{\mathrm{t0}} := [u_{1,t0}^*, u_{2,t0}^*, u_{3,t0}^{**}]$, to the system (3-2).
4:	Measure the state and update the parameter.
5:	Go to step 2.

3-5 Numerical study

We consider a building (zone) with the characteristics and modeling parameters shown in Appendix C. This building does not represent any particular building, and is rather the result of the mathematical equations from Section 2-4. The sampling time $\Delta t = 15$ [min], the simulation time $T_{\mathrm{sim}} = 24$ [hr] equals 96 steps and the prediction horizon N_{p} =5 [hr] equals 20 steps.

The day analyzed was August 29, 2016 from 5:00 am. Its weather conditions were taken from [35], and contained information of the outside ambient temperature, humidity ratio, and solar radiation, Figure C-3. The prediction of the sensible, latent disturbances and occupancy profile are shown in Figure C-1. The two former were obtained by using the equations from Section 2-4, and the profile of the number of people was taken from [36]. This occupancy

pattern was scaled down accordingly to the 200 [m^2] zone area dimensions, and it was chosen sufficiently high to produce significant effects on temperature and humidity of the zone. In addition, we include the analysis of the case 3 controller for September 13, 2016 from 5:00. These day is a warmer and more humid day, as shown in figure C-4, The prediction of the heat disturbances are illustrated in C-2.

The simulations were initialized with the building zone temperature x_1 at 23 [°C] and a humidity ratio x_2 at 12 [$g_w kg_a^{-1}$]. The optimization problem from (3-21) was solved using Yalmip as the interface and 'SQP' as the solver, [37]. This gradient-based solver automatically calculates the solution by using the Sequential Quadratic Programming numerical method. The initial guess for the nonlinear MPC was left to the solver, thus, it looks at the bounds and initializes the variables inside these bounds.

Each of the following sections presents the control in temperature and humidity ratio of the zone using MPC.

First, we analyze the effects on the humidity ratio when the temperature of the zone T_z is the only controlled state and the control inputs from the supply air are its mass flow rate $\dot{m}_a$ and its temperature T_{sa}. Then, we present the MPC problem formulation for temperature and humidity control, in which the objective function has two goals, namely the energy minimization of the cooling and heating coils and the reference tracking problem in temperature and humidity ratio of the zone. In this formulation, we discuss three cases that differ in the energy minimization term of the objective function. These terms are the air mass flow rate, the energy from ventilation and the enthalpy of the system. We also show the performance of case 3 controller.

Of course, in general the optimization goals stated in (3-3-4) should be met for the stated formulations. However, it is hard to quantify the benefits without a reference controller (or recorded performance data) to compare it to. Therefore, the MPC from Section 3-5-2 is taken as the reference controller.

3-5-1 Effects on the humidity ratio for temperature control only

We solve the problem from (3-21) for the constraints and dynamics corresponding to the temperature only, which yields to the nonlinear MPC formulation:

$$\min_{\boldsymbol{u}} \quad \sum_{k=0}^{N_p} J(\boldsymbol{x},\boldsymbol{u}) = \|y_{1,k} - T_{sp}\|^2_{Q_T} + ||u_1||^2_{Q_u} + \rho_1\epsilon_1 \tag{3-28a}$$

$$\text{s.t.} \quad x_{1,k+1} = x_{1,k} + \Delta T\left(k_{1,z}u_{1,k}(u_{2,k} - x_{1,k}) + k_{2,z}(d_{1,k} - x_{1,k}) + k_{3,z}d_{2,k}\right) \tag{3-28b}$$

$$\forall k = 0, 1, \cdots, N_p - 1$$

$$y_k = x_{1,k},\ \forall k = 0, 1, \cdots, N_p - 1 \tag{3-28c}$$

$$\underline{T_z} - \epsilon_2 \leq y_k \leq \overline{T_z} + \epsilon_1,\ \forall k = 1, 2, \cdots, N_p \tag{3-28d}$$

$$\underline{T_{sa}} \leq u_{2,k} \leq \overline{T_{sa}},\ \forall k = 0, 1, \cdots, N_p - 1 \tag{3-28e}$$

$$\underline{m_{sa}} \leq u_{1,k} \leq \overline{m_{sa}},\ \forall k = 0, 1, \cdots, N_p - 1 \tag{3-28f}$$

$$\epsilon_1, \epsilon_2 \geq 0 \tag{3-28g}$$

To show the effects on the humidity ratio of the zone (3-29), we will analyze the air conditioning processes that are required to achieve the supply air temperature $u_2 = T_{sa}$, which is

a solution of (3-28). The supply air humidity ratio $u_3 = W_{\text{sa}}$ in this section is not controlled, but rather is a consequence of the air conditioning processes in the coils. The results of the simulation are shown in Figure 3-3 and Figure 3-4.

Humidity ratio in the zone

This dynamics (3-29) are affected by ventilation and by the air conditions. The former expressed as the air mass flow rate $u_1 = \dot{m}_{\text{a}}$, which is a solution from (3-28), and the latter by the air humidity ratio $u_3 = W_{\text{sa}}$.

$$x_{2,k+1} = x_{2,k} + \Delta T(k_{4,\text{z}} u_{1,k}(u_{3,k} - x_{2,K}) + k_{4,\text{z}} d_{3,k}) \tag{3-29}$$

The humidity ratio of the supply air $u_3 = W_{\text{sa}}$, which is an uncontrolled input for this section, is computed by analyzing the processes that may occur due to the air conditioning requirements with respect to the temperature of the supply air T_{sa}. These processes are heating, cooling and cooling and dehumidification, which are explained next.

Relative Humidity in the zone

With the knowledge of $x_1 = T_{\text{z}}$ and $x_2 = W_{\text{z}}$, we can compute the RH_{z} using (A-9). The nonlinear formula of the relative humidity can mathematically be greater than 100%, which is an unrealistic concept. A value of 100% physically means that the air cannot longer hold more water vapor, thus, liquid water appears. To make the system more realistic, when the relative humidity RH_{z} is greater than 100%, we compute the humidity ratio of the zone W_{z} from the approximation of the curve at $RH = 100\%$ as follows:

$$W_{\text{z}} = aT_{\text{z}}^2 + bT_{\text{z}} + c, \tag{3-30}$$

where $T_{\text{z}} = x_1$ and the coefficients a, b and c are constant parameters obtained by using the nonlinear least-square method from Section 2-3-5.

Temperature and humidity ratio of the coils

While the only controlled variable is the zone temperature T_{z}, the operation of the cooling and heating coils is exclusive. This allows us to determine whether cooling or heating is required by the knowledge of the supply air temperature T_{sa}.

Heating: It occurs when the supply air temperature is greater than the mixed air. These conditions are expressed as:

$$T_{\text{sa}} \geq T_{\text{ma}}$$

The air temperature and humidity ratio of the coils are then expressed as:

$$T_{\text{cc}} = T_{\text{ma}} \tag{3-31a}$$
$$W_{\text{cc}} = W_{\text{ma}} \tag{3-31b}$$
$$T_{\text{hc}} = T_{\text{sa}} \tag{3-31c}$$
$$W_{\text{sa}} = W_{\text{hc}} = W_{\text{ma}} \tag{3-31d}$$

Cooling: It occurs when the supply air temperature is less than the mixed air and greater than the dew point temperature of the mixed air. These conditions are expressed as:

$$T_{\text{sa}} < T_{\text{ma}} \wedge T_{\text{sa}} > T_{\text{d,ma}}$$

The air temperatures and humidity ratios of the coils then yield to:

$$\begin{aligned} T_{\text{cc}} &= T_{\text{sa}} && \text{(3-32a)} \\ W_{\text{cc}} &= W_{\text{ma}} && \text{(3-32b)} \\ T_{\text{hc}} &= T_{\text{cc}} && \text{(3-32c)} \\ W_{\text{sa}} = W_{\text{hc}} &= W_{\text{ma}} && \text{(3-32d)} \end{aligned}$$

Cooling and dehumidification: It occurs when the supply air temperature is less than the mixed air and its dew point temperature. While there is no control of the humidity is this section and the coils operate exclusively, the re-heating process is disregarded. Then, the condition for this process is expressed as:

$$T_{\text{sa}} < T_{\text{ma}} \wedge T_{\text{sa}} \leq T_{\text{d,ma}}$$

The air temperatures and humidity ratios of the heating and cooling coils are:

$$\begin{aligned} W_{\text{cc}} &= aT_{\text{sa}}^2 + bT_{\text{sa}} + c && \text{(3-33a)} \\ T_{\text{cc}} &= T_{\text{sa}} && \text{(3-33b)} \\ T_{\text{hc}} &= T_{\text{sa}} && \text{(3-33c)} \\ W_{\text{sa}} = W_{\text{hc}} &= W_{\text{cc}} && \text{(3-33d)} \end{aligned}$$

(3-31), (3-32) and (3-33) allows us to compute the cooling and heating coils heat transfers and energies using the relation from (3-27).

Discussion of the results

In Figure 3-3 and Figure 3-4, we aim to show the effects on the humidity when the temperature of the zone is the only controlled variable. In these illustrations, the upper plot depicts the temperature $x1 = T_{\text{z}}$, the middle plot the dynamics of the humidity ratio $x_2 = W_{\text{z}}$ and the bottom plot the relative humidity in the zone RH_{z}. The initial condition for Figure 3-3 is $x_0 = [23, 12]$ and for Figure 3-4 is $x_0 = [23, 7]$. The bounds for each of these variables are indicated with dashed lines.

Figure 3-3 and 3-4 reveal that the sole control of temperature does not guarantee that the humidity ratio of the zone W_{z} remains within bounds when the zone is subjected to high occupancy and an uncontrolled humidity ratio from ventilation W_{sa}. For instance, the disturbances in the initial time step and during the time step 29,10:00 and 29,18:00 from Figure C-1 affect significantly the humidity in the zone. Furthermore, there are also seen values of the relative humidity in the zone RH_{z} greater than 100%. This situation is explained by the fact that we used the mathematical equation of the relative humidity (A-9) and the approximation of the humidity ratio of the zone W_{z} for values greater than 100%, (3-30).

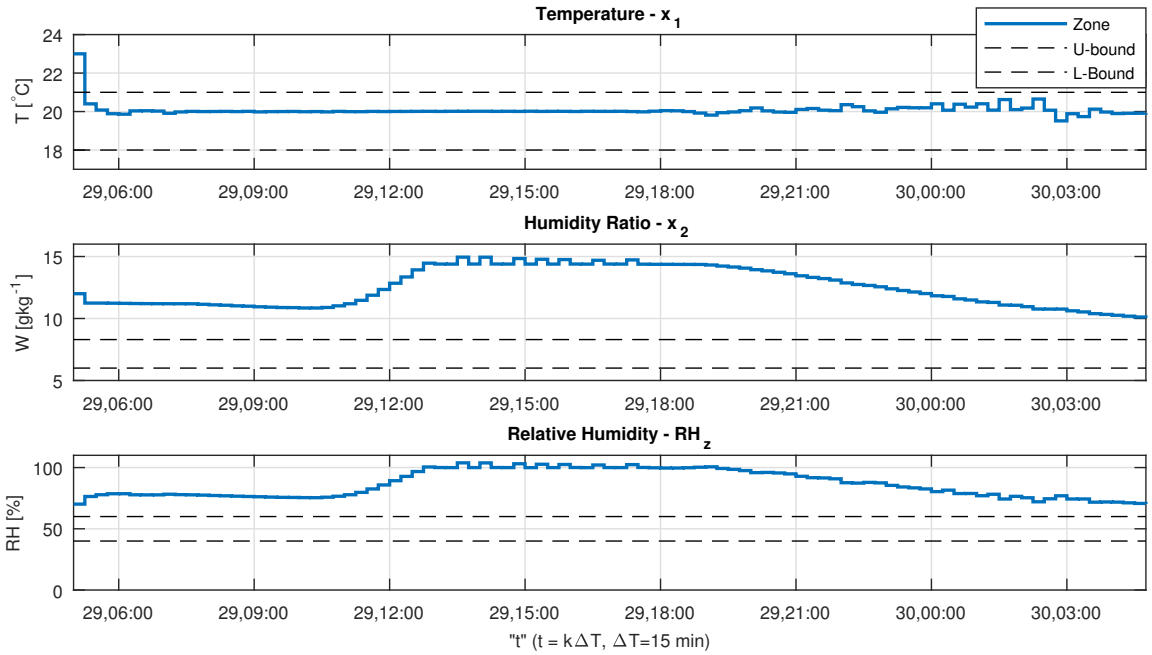

Figure 3-3: Building MPC temperature control and the effects on the humidity - Initial condition $x_0 = [23, 12]$

Figure 3-3 also shows that an initial condition of $x_0 = [23, 12]$, where the humidity ratio is off-bounds, leads to the violation of the humidity bounds for the whole simulation time. Herein, ventilation is not able to steer the humidity to its bounds even when the moisture from occupancy is zero.

Figure 3-4 shows that the initial condition $x_0 = [23, 7]$ keeps the humidity relatively stable within bounds before time step 29,11:00. During this period, the ventilation system does not have a significant impact on the humidity inside the zone. Nevertheless, humidity experiences a gradual increase as occupancy rises occasioning the violation of the bounds for the rest of the simulation. Even though after 29,18:00 the moisture from occupancy does not longer affect the zone, the ventilation system does not remove enough moisture out of the zone to satisfy the humidity limits.

The previous findings demonstrate that to guarantee climate comfort when the zone is subjected to considerable moisture disturbances we need to perform the joint control of temperature and humidity.

3-5-2 Joint control in temperature and humidity ratio

In this section we present the nonlinear MPC control of temperature and humidity ratio of the zone. We have previously shown that performing the single control of temperature disregarding humidity compromises climate comfort whenever the moisture disturbances are significant. To overcome this issue, we introduce the following optimization problem based

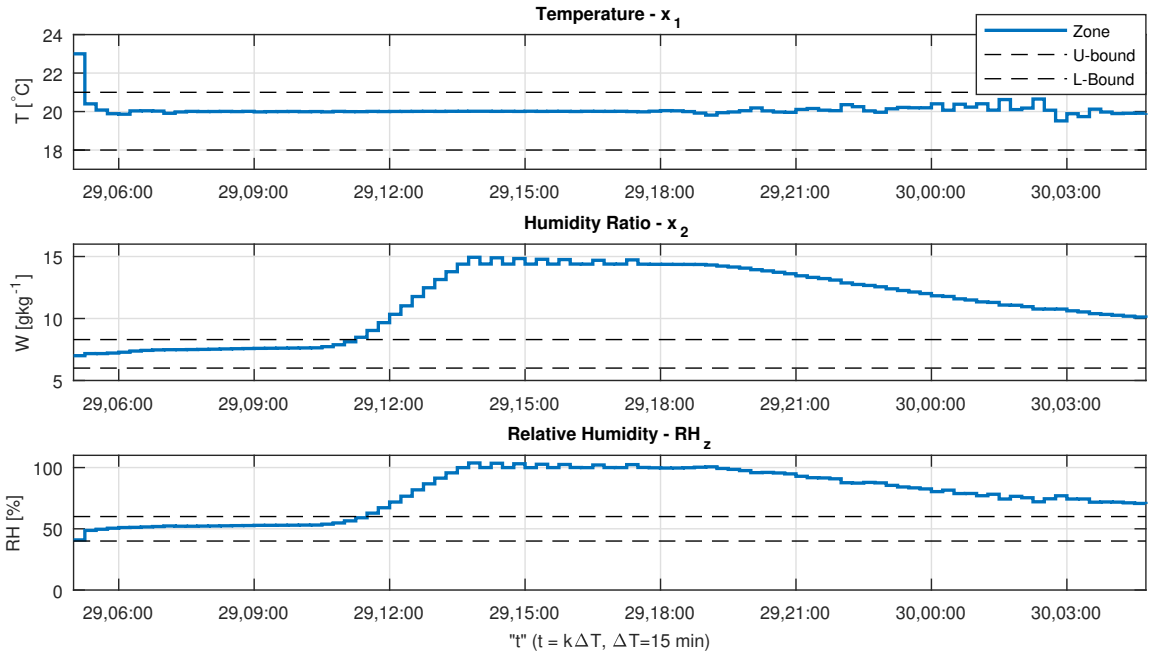

Figure 3-4: Building MPC temperature control and the effects on the humidity - Initial condition $x_0 = [23, 7]$

on our developments from Section 3-4:

$$\min_{\boldsymbol{u}} \quad \sum_{k=0}^{N_\mathrm{p}} \left(J(\boldsymbol{x}, \boldsymbol{u}) + \sum_{i=1}^{2} \rho_i \epsilon_i \right) \tag{3-34a}$$

$$x_{1,k+1} = x_{1,k} + \Delta T \left(k_{1,\mathrm{z}} u_{1,k} (u_{2,k} - x_{1,k}) + k_{2,\mathrm{z}} (d_{1,k} - x_{1,k}) + k_{3,\mathrm{z}} d_{2,k} \right), \quad \forall k = 0, 1, \cdots, N_\mathrm{p} - 1 \tag{3-34b}$$

$$x_{2,k+1} = x_{2,k} + \Delta T (k_{4,\mathrm{z}} u_{1,k} (u_{3,k} - x_{2,K}) + k_{4,\mathrm{z}} d_{3,k}), \ \forall k = 0, 1, \cdots, N_\mathrm{p} - 1 \tag{3-34c}$$

$$y_k = C x_k, \ \forall k = 0, 1, \cdots, N_\mathrm{p} - 1 \tag{3-34d}$$

$$\underline{x_\mathrm{z}} - \begin{bmatrix} 1 \\ 1 \end{bmatrix} \epsilon_2 \leq y_k \leq \overline{x_\mathrm{z}} + \begin{bmatrix} 1 \\ 1 \end{bmatrix} \epsilon_1, \ \forall k = 1, 2, \cdots, N_\mathrm{p} \tag{3-34e}$$

$$\underline{m_\mathrm{sa}} \leq u_{1,k} \leq \overline{m_\mathrm{sa}}, \ \forall k = 0, 1, \cdots, N_\mathrm{p} - 1 \tag{3-34f}$$

$$\underline{T_\mathrm{sa}} \leq u_{2,k} \leq \overline{T_\mathrm{sa}}, \ \forall k = 0, 1, \cdots, N_\mathrm{p} - 1 \tag{3-34g}$$

$$\underline{W_\mathrm{sa}} \leq u_{3,k} \leq \overline{W_\mathrm{sa}}, \ \forall k = 0, 1, \cdots, N_\mathrm{p} - 1 \tag{3-34h}$$

$$\epsilon_1, \epsilon_2 \geq 0 \tag{3-34i}$$

(3-34) solves the reference tracking of the states $x = [T_\mathrm{z}, W_\mathrm{z}]^\top$, and the energy minimization problem. Here, the relative humidity in the zone RH_z is indirectly controlled by tracking the desired set-points and satisfying the bounds in the zone temperature and humidity ratio, which allows the relative humidity RH_z to fluctuate around the values defined in Section 3-3-5. The energy minimization problem is represented by three scenarios.

The constraints of (3-34) correspond to the system dynamics, state constraints and input constraints. The former is represented by the discrete-time equations (3-34b) and (3-34c).

The states constraints are the upper and lower limits in temperature $x_1 = T_z$ and humidity ratio $x_2 = W_z$ of the zone, (3-34e). The input constraints correspond to the air conditioning inputs, namely, $u = [m_{sa}, T_{sa}, W_{sa}]^\top$, (3-34g) to (3-34h). The slack variables constrains are defined in (3-34i)

Case 1: Reference tracking and mass flow rate formulation

In this scenario, we aim to optimize the heat transfers of the cooling and heating coils by minimizing the air mass flow rate. The problem (3-34) has the following cost function:

$$J(\boldsymbol{x}, \boldsymbol{u}) = \|y_k - x_{sp}\|^2_{Q_y} + \|u_1\|^2_{Q_u} + \rho_1\epsilon_1 + \rho_2\epsilon_2, \tag{3-35}$$

This goal was chosen since the energy across the coils can be expressed as:

$$\dot{Q} = c_a \dot{m}_a \Delta T, \tag{3-36}$$

where c_a is the specific heat capacity of the air, $\dot{m}_a$ the air mass flow rate and ΔT the air temperature difference across the coil. This relation allows us to have an indirect control of the heat rate of the coils.

In this formulation, the cost function is a multi-objective function described by a quadratic cost function of the deviation between the states and their set-points, and a quadratic cost function of the air mass flow rate input. These costs are weighted by the matrices $Q_{\mathbf{y}}$, and Q_u, which were chosen iteratively. The weights ρ_1 and ρ_2 were chosen sufficiently large. The results from this problem are presented in Figure 3-5, Figure 3-8 and Figure 3-13.

Case 2: Reference tracking and sensible heat formulation

(3-34) is solved considering the reference tracking problem of the states, as explained in the previous sections, and the energy problem in terms of the air conditioning inputs, namely the air mass flow rate u_1 and the supply air temperature u_2, which corresponds to the sensible heat transfer through ventilation. The cost function yields to:

$$J(\boldsymbol{x}, \boldsymbol{u}) = \|y - x_{sp}\|^2_{Q_y} + \|u_1\|^2_{Q_u} + \tau u_1 c_a |u_2 - x_1| + \rho_1\epsilon_1 + \rho_2\epsilon_2 \tag{3-37}$$

Note that the cost function includes, with the third term of equation (3-37), a cost on the absolute difference of the temperature of the supplied air and the temperature of the air of the zone, which corresponds to the heat by ventilation. This term is different from that of the heat transfers of the coiling or of the heating coils.

Similar to the previous case, the cost function is a multi-objective function described by (3-35) and the linear cost from the sensible heat transfer by ventilation, third term in (3-37). The costs are weighted by the matrices Q_y, Q_u, and τ, which were chosen iteratively. The weights ρ_1 and ρ_2 were chosen sufficiently large. The results from this problem are presented in Figure 3-6, Figure 3-9 and Figure 3-14.

In addition, in this section we support the difference between the heat transfers from the coils and ventilation in Figure 3-11 and Figure 3-12. In these figures, the heat from ventilation is computed from:

$$\dot{Q}_{vent} = c_a u_1 (u_2 - x_1), \tag{3-38}$$

where heating from ventilation corresponds to its positive part, while the cooling to its negative values.

Case 3: Reference tracking and enthalpy formulation

This formulation considers the reference tracking problem of the states and the energy problem expressed in terms of the enthalpy the system, which was analyzed in Section 2-3. The cost function yields to:

$$\begin{aligned} J(\boldsymbol{x},\boldsymbol{u}) &= \|y_k - x_{\mathrm{sp}}\|^2_{Q_\mathrm{y}} + \|u_1\|^2_{Q_\mathrm{u}} + \tau\dot{m}_\mathrm{a}\,|c_\mathrm{a}T_\mathrm{sa} + h_\mathrm{wv}W_\mathrm{sa} - (c_\mathrm{a}T_\mathrm{ma} + h_\mathrm{wv}W_\mathrm{ma})| \quad (3\text{-}39) \\ & \quad \rho_1\epsilon_1 + \rho_2\epsilon_2 \end{aligned}$$

This cost function is a multi-objective function described by (3-35) and the linear cost from the enthalpy throughout the air conditioning process, third term in (3-39). The costs are weighted by the matrices Q_y, and Q_u, and τ, which were chosen iteratively. The weights ρ_1 and ρ_2 were chosen sufficiently large. The results from this problem are presented in Figure 3-7, Figure 3-10 and to Figure 3-15.

Discussion of the results

For each of the cases from Section 3-5-2, the figures 3-5, 3-6 and 3-7 illustrate the temperature, the humidity ratio and the relative humidity of the *zone*; the figures 3-8, 3-9 and 3-10 show the air mass flow rate, temperature and humidity ratio of the *supply air*. The bounds for each of these variables are indicated with dashed lines.

The figures 3-13, 3-14 and 3-15 present the heat transfers across the coils and the cumulative energy loads of each of those coils. The figures 3-11 and 3-12 indicate the heat transfers for cooling and heating produced by *ventilation* in comparison to the heating and cooling *loads* of the coils. Here, the red color is associated to the heating coil, blue color to the cooling coil, and black to heating or cooling by ventilation. The initial condition for each case is $x_0 = [23, 12]$.

As can be seen from the figures 3-5, 3-6 and 3-7, the reference tracking problem in temperature x_1 and humidity ratio x_2 of the zone allows to have an indirect control on the relative humidity in the zone RH_z, which is demonstrated by the fairly stable response of this variable within its bounds.

The optimal supply air inputs of the air conditioning system shown in the figures 3-8, 3-9 and 3-10 indicate that the relation among them is not a straightforward concept for the whole simulation time and the provided prediction of the disturbances from figure C-1. The optimal air mass flow rate u_1 is kept low, and it causes a fluctuating effect on the temperature u_2 and humidity ratio u_3 of the supply air. While a decrease in temperature of the supply air u_2 occurs at around 29,8:00 in case 1 and 3 thus anticipating almost two hours in advance the sharp increase of the latent and heat gains at time 29,10:00, the humidity ratio of the supply air u_3 does not show an anticipating trend nor the humidity ration $u2$ from case 2. In all the cases, u_3 shows a relative stable trend around its maximum limit whenever the moisture gains are insignificant. For instance during the off-peak hours of occupancy, especially after

the time 29,18:00. This behavior demonstrates how the controller in each tries to compensate the sensible and latent heats in the zone.

Figure 3-11 and 3-12 showcase the difference between the heat by ventilation that is transferred to the zone and the heat that is injected by the cooling and heating coils to the system. Figure 3-11 demonstrates that the heat for both cases is indeed higher during the dehumidification periods from 29,10:00 to 29,18:00 and at the beginning of the simulation. However, the ventilation heat used for cooling the zone is almost negligible in comparison to the heat of the cooling coil. A similar behavior is shown in figure 3-12, where the ventilation heat for heating the zone is not considerable with respect to the heat injected by the heating coil. Here, the heat injected by the heating coil corresponds to the re-heating process and we observe it accounts to significant values. These observations prove that if we use solely the heat from ventilation as the heating or cooling demand of a building, we fall into downsizing the water side system requirements.

From Figure 3-13, 3-14 and 3-15, two main outcomes were found. First, more heat is required for dehumidification, especially for the periods from time 29,10:00 to 29,18:00 and at the beginning of the simulation. During these periods simultaneous cooling and heating of the air is required thus resulting in higher energy consumption. As dehumidifying the air entails not only sensible cooling but also latent cooling, the amount of energy required to change the phase of the air shows a substantial increase in comparison to the periods where dehumidification is not needed. In addition, the heat from the re-heating process that compensates the sensible loss during dehumidification causes a significant increase in the total heat transfers.

The second outcome regards the energy consumption for that day, which is shown in tables 3-2 and 3-3. In table 3-2 we observe that the fan energy is negligible in comparison to the cooling and heating coil energies for the three cases, and that the cooling and heating energies are similar. Moreover, from 3-3 case 2 shows a decrease of 1.00% in comparison to the base line strategy (case 1) confirming that improvement in energy usage exists when the heat from ventilation is taken into account in the objective function of the MPC formulation. Finally, a further improvement of 5.82% is accomplished by the energy problem formulated in terms of enthalpy, case 3. This last improvement is the consequence of incorporating the enthalpy of the whole system into the problem formulation.

In addition, even though the focus of this work is not an economic approach, roughly speaking, if we considered the price of electricity at around 18 euro cents per kWh, the price for each case is 13.80, 13.67 and 13.00 euros a day. This shows the economic benefits on a daily basis.

Table 3-2: Total energy consumption of the system for Aug 29, 2016

Case of study / Equipment	Energy [kWh]		
	1(Baseline)	**2**	**3**
Cooling coil	43.00	43.02	41.58
Heating coil	33.69	32.90	30.64
Fan	0.116	0.117	0.104

Figure 3-16 shows climate comfort is also achieved when the system is subjected to warmer and more humid conditions. Figure 3-17 demonstrates how the energy consumption of the system rises up to 88.25 [kWh] while the cooling and heating coils energy also increases up to

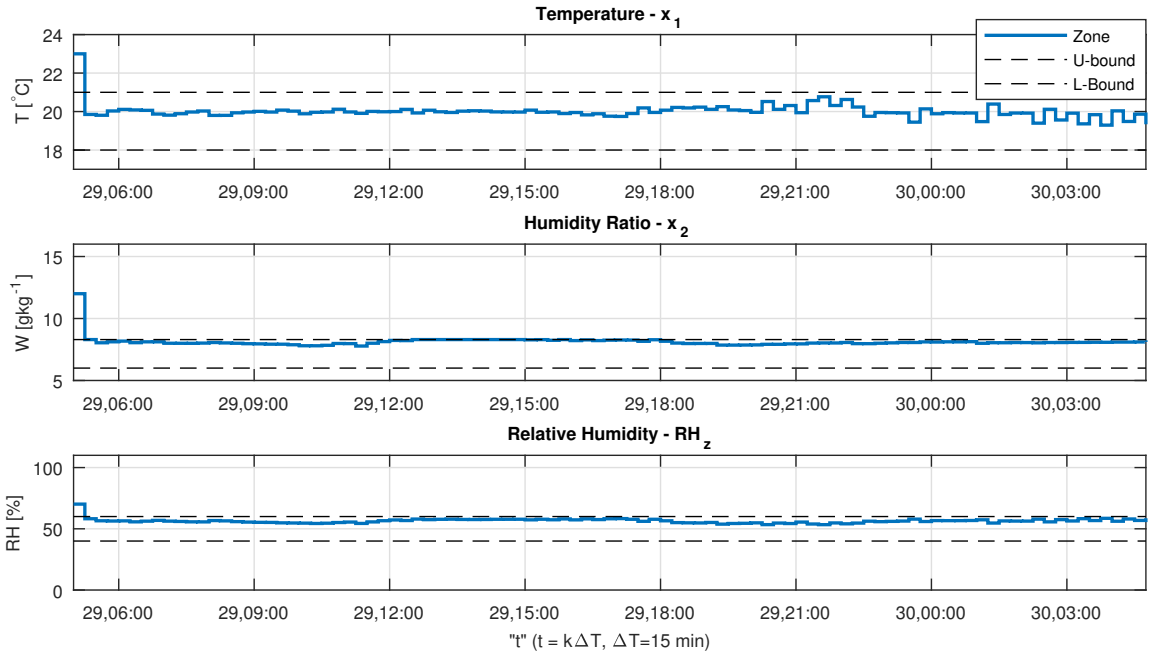

Figure 3-5: Building MPC temperature and humidity ratio control - case 1: States evolution and the relative humidity in the zone

61.55 [kWh] and 25.40 [kWh]. As seen in the figure C-4, the day is more humid causing the cooling coil to remove more moisture out from the air thus more energy is required.

Table 3-3: Total energy consumption of the coils and fan, and the energy percentage reduction in each case of study for Aug 29, 2016

Performance indicator	**Case of study**		
	1(Baseline)	**2**	**3**
Energy (kWh)	76.80	76.04	72.33
Energy reduction (%)	-	1.00	5.82

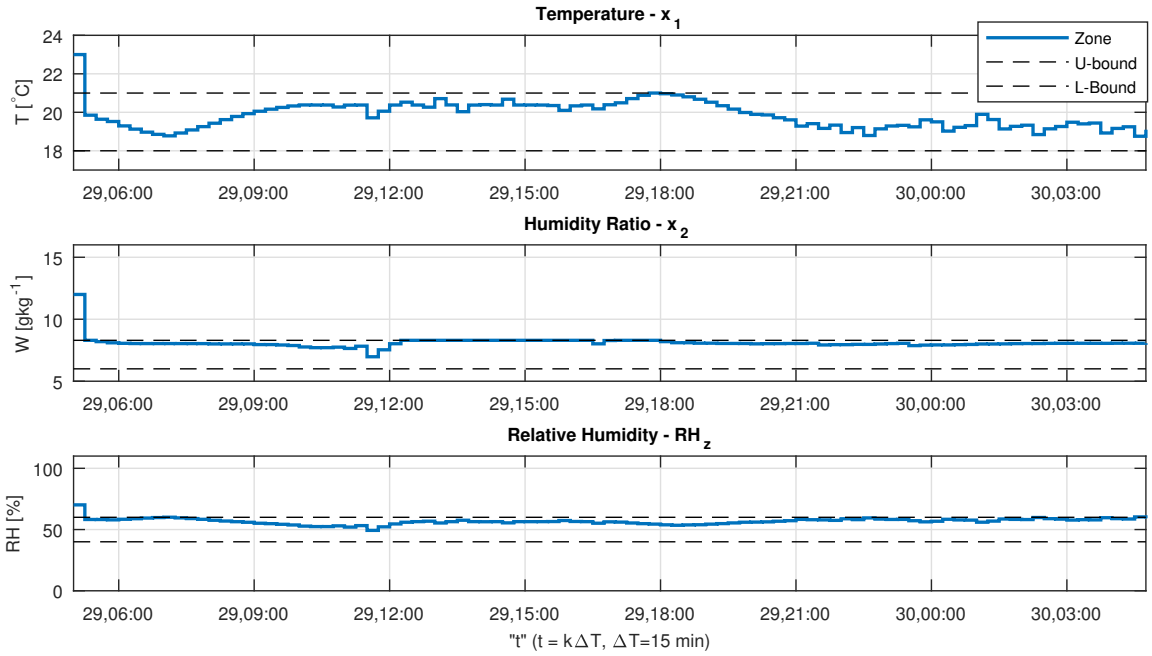

Figure 3-6: Building MPC temperature and humidity ratio control - case 2: States evolution and the relative humidity in the zone

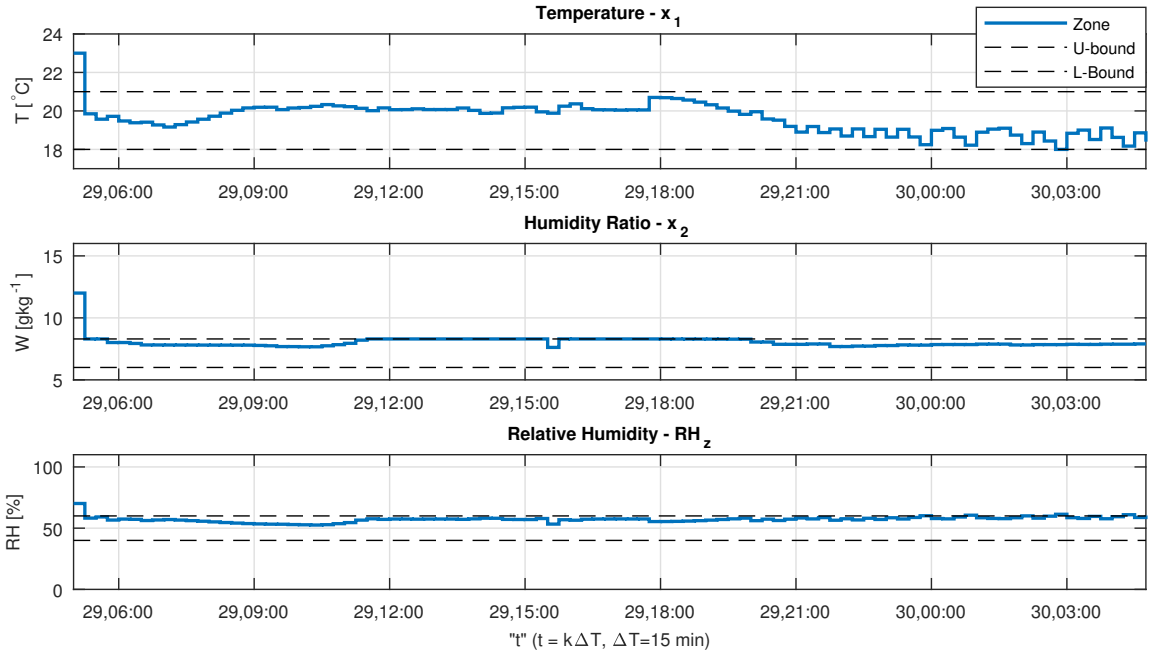

Figure 3-7: Building MPC temperature and humidity ratio control - case 3: States evolution and the relative humidity in the zone

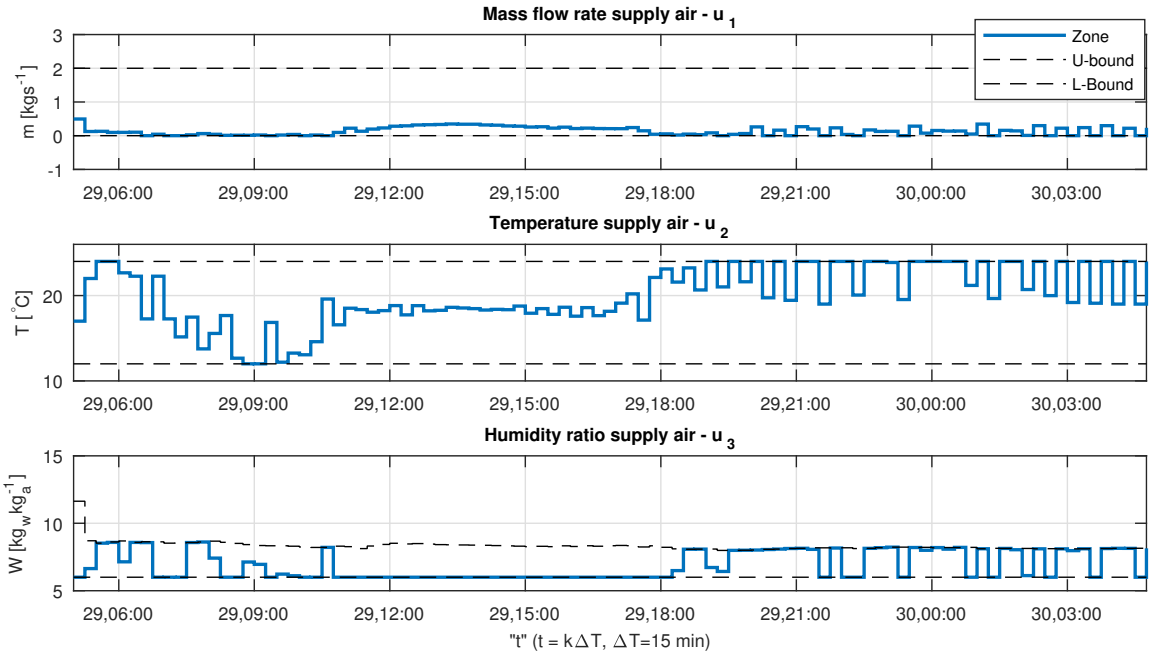

Figure 3-8: Building MPC temperature and humidity ratio control - case 1: Supply air inputs

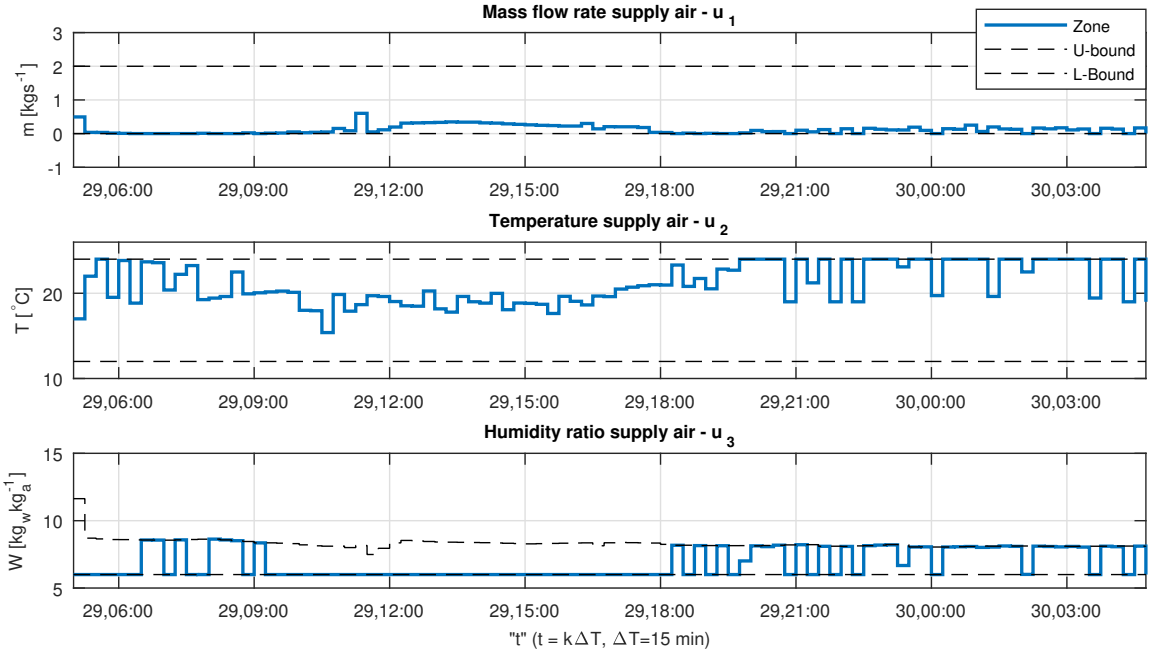

Figure 3-9: Building MPC temperature and humidity ratio control - case 2: Supply air inputs

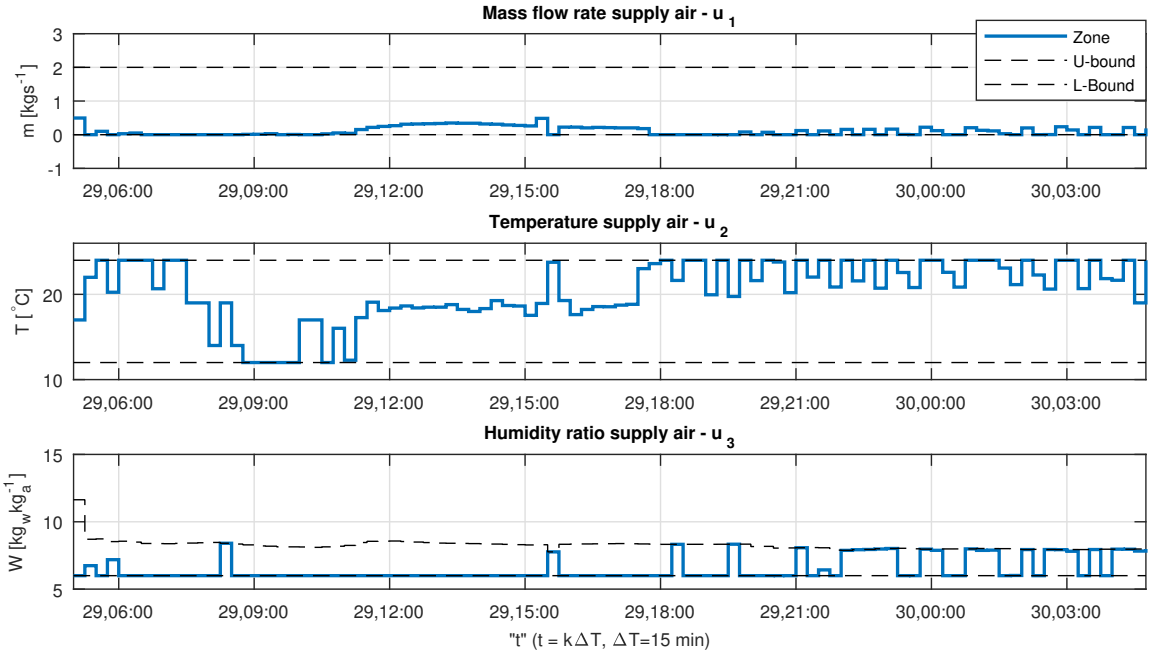

Figure 3-10: Building MPC temperature and humidity ratio control - case 3: Supply air inputs

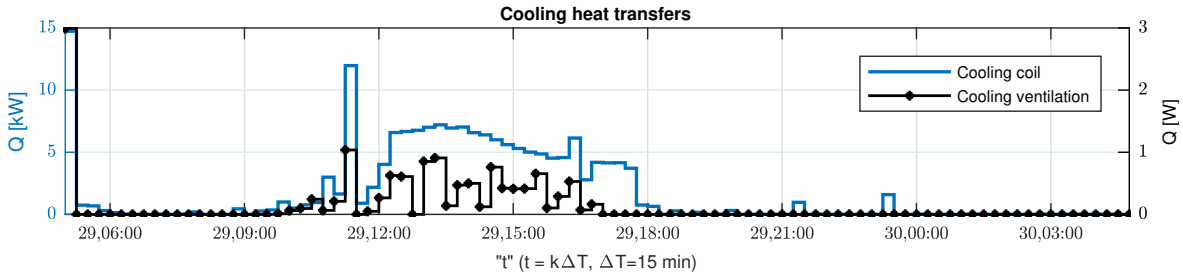

Figure 3-11: Building MPC temperature and humidity ratio control - case 2:- Cooling coil and ventilation heat transfers

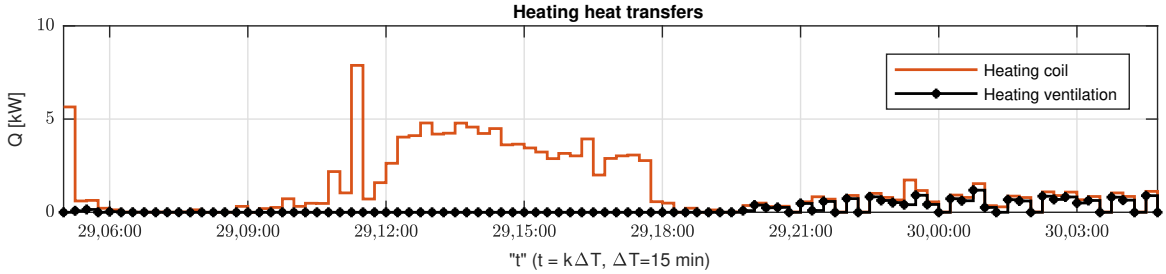

Figure 3-12: Building MPC temperature and humidity ratio control - case 2:- Heating coil and ventilation heat transfers

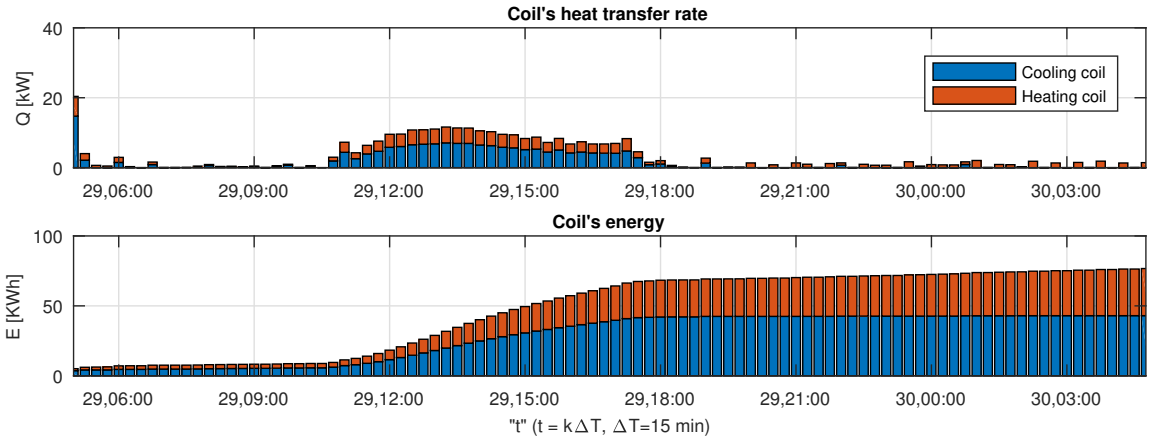

Figure 3-13: Building MPC temperature and humidity ratio control - case 1: Heat transfer rate and the cumulative energy of the coils

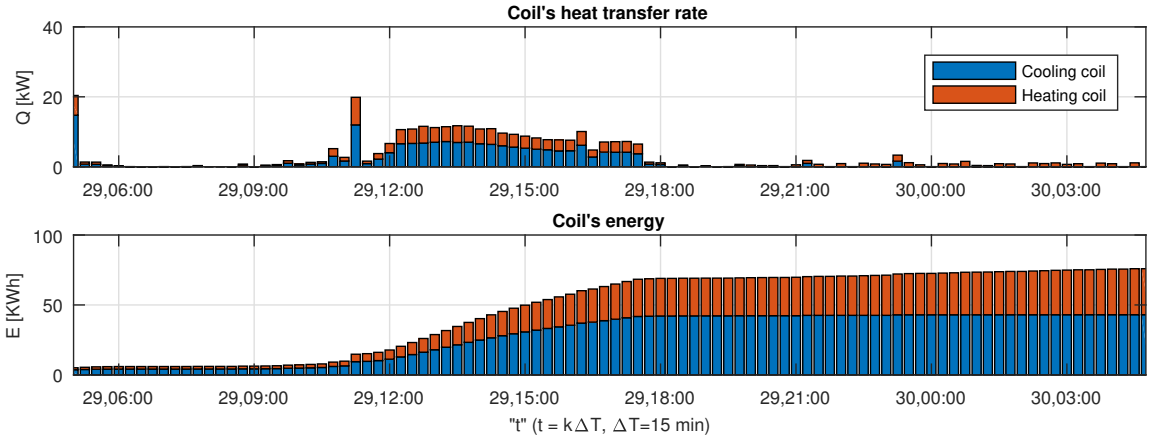

Figure 3-14: Building MPC temperature and humidity ratio control - case 2: Heat transfer rate and the cumulative energy of the coils

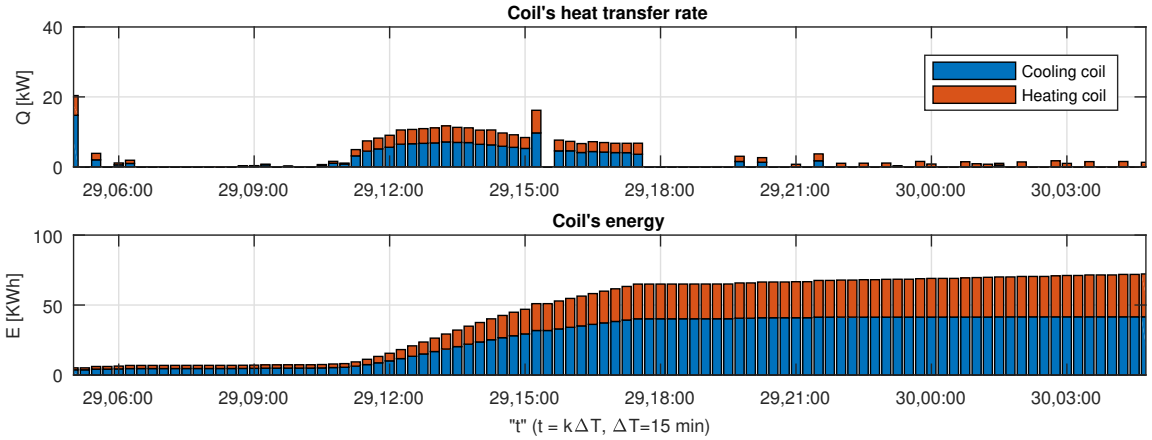

Figure 3-15: Building MPC temperature and humidity ratio control - case 3: Heat transfer rate and the cumulative energy of the coils

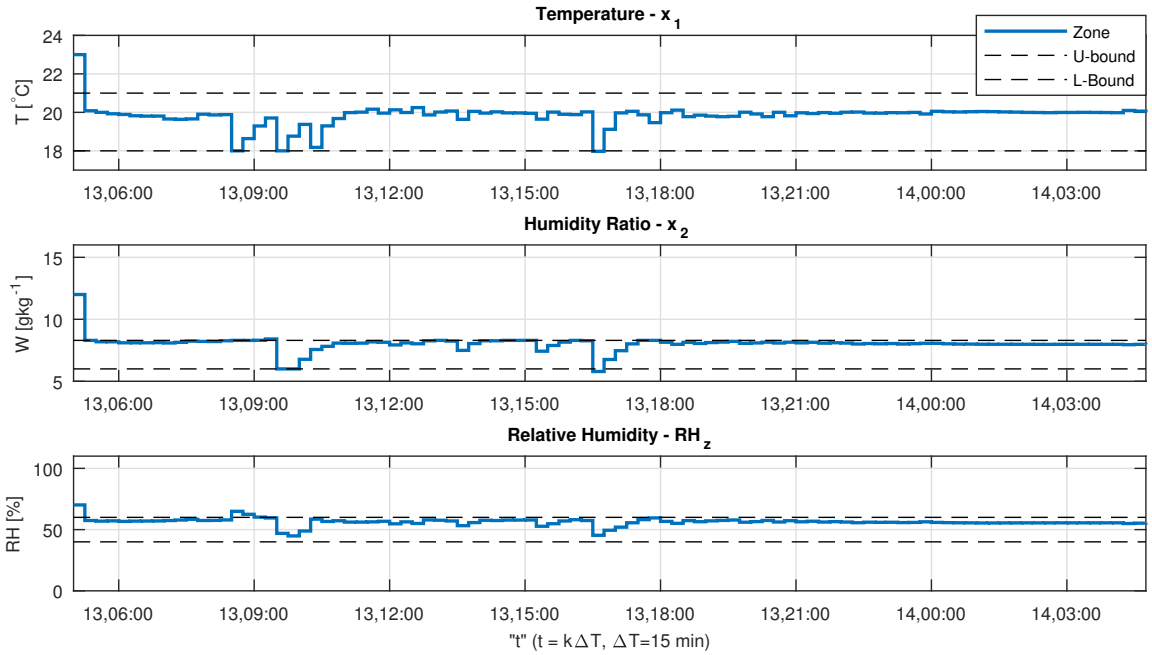

Figure 3-16: Building MPC temperature and humidity ratio control - case 3: States evolution and the relative humidity in the zone for September 13, 2016

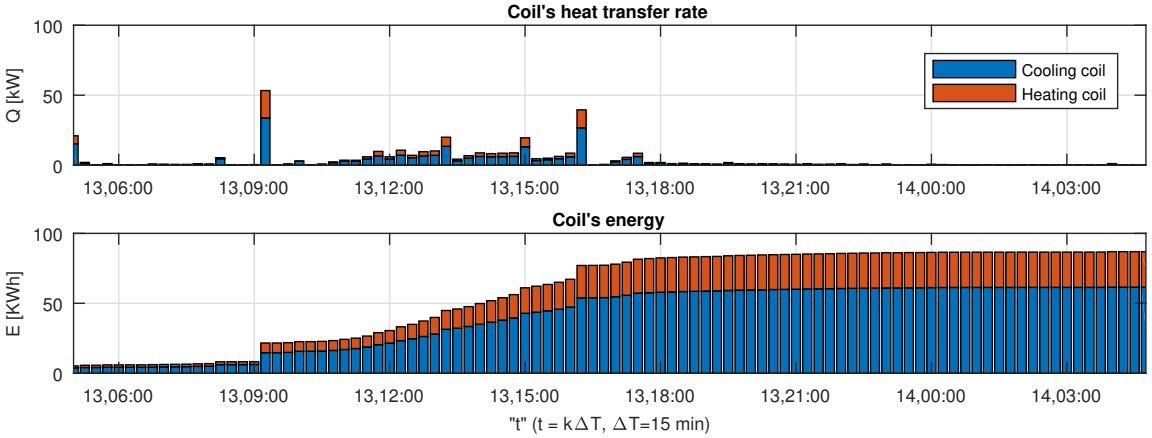

Figure 3-17: Building MPC temperature and humidity ratio control - case 3: Heat transfer rate and the cumulative energy of the coils for September 13, 2016

Chapter 4

Conclusions and recommendations

The focus of this research is to develop a MPC approach for cooling and dehumidification in buildings, where the processes are controlled by cooling and heating coils as the main air conditioning units. This final chapter presents the conclusions from these developments, and gives recommendations for future work.

4-1 Conclusions

Every control system needs a representative model of the dynamics of the engineering system. In this thesis, the modeling yielded a nonlinear system, where the states were the temperature and humidity ratio in the zone, and the inputs were the air mass flow rate, the supply air temperature and the supply air humidity ratio. This simplified modeling of the dynamics disregarded the complex dynamics of the coils, and allowed us to define the set-points of the coils in terms of the supply air temperature and humidity ratio.

The air conditioning psychrometric analysis of the studied system enabled us to support the aforementioned modeling simplification by establishing the heat transfers in terms of the mixed air and the supply air temperature and humidity ratio. This allowed us to determine how much heat and thermal energy is required by the coils at each sampling time. However, it should be pointed out that the evolution of the air temperature and humidity in the coils are nonlinear processes and their dynamics were not included for the studied case due to the complexity it adds to the problem, and due to the unavailability of data to realize a realistic sizing of the coils.

The simplified dynamics laid the basis for the MPC controller formulation, in which we studied three approaches that differ by the cost function defined. The main advantage of using this controller is the optimization over a prediction horizon instead of a single step. This allows to take uncertainty into account. On the other hand, the prediction horizon is a variable that increases the number of decision variables to be optimized, and thus the computational effort of the problem. Here, a trade-off had to be made between the system prediction accuracy

and the complexity of the resulting optimization problem considering we posed the system as a nonlinear system.

We investigated three scenarios in terms of the reference tracking problem and the energy minimization problem. This energy minimization focused on optimization with respect to the air mass flow rate, the air mass flow rate and the sensible heat from ventilation, and the air mass flow rate the enthalpy of the system. Here, we demonstrated that the sensible heat from ventilation is not the heat produced by the coils, especially during the dehumidification process. Although the use of the sensible term in the cost function showed an improvement in energy usage in comparison to the mass flow control formulation, these two concepts must not be confused. The decrease in the energy usage is the result of the air conditioning process, as shown in the psychrometric analysis of the air.

For each scenario, we proposed to solve the nonlinear constrained optimization problem with state and input constraints. To solve the nonlinear program, we use the toolbox Yalmip in Matlab and the Sequential Quadratic Programming (SQP) solver. The toolbox supplies the warm-starting for the optimization problem inside the bounds defined then it computes the solution. The results from these approaches confirm the comfort requirements, and energy reduction is also confirmed. The results that included the enthalpy variation showed an improvement in terms of energy usage. However, we encountered difficulties tuning the weights in the cost function to reach those results.

4-2 Future work

In order to improve the present project, the following tasks are suggested.

The major area that requires further investigation is the modeling of the system dynamics, especially with respect to humidity and the factors influencing its variation. For instance infiltrating moisture from the outside weather conditions, moisture absorption or desorption in built-in materials of the construction, or building defects (piping leaks, rain penetration, envelope cracks).

Another aspect of improvement is the development of the forecasting occupancy and weather models. In this study, they have been considered to be deterministic and available. However, in reality these uncertainties are stochastic processes characterized by non Gaussian distributions. Thus, the controller synthesis needs to address this behavior.

It is also suggested to carry out system identification and filtering techniques of a similar system to prove the theoretical results of the controller. This can be done by means of a dedicated energy simulation software for buildings or by studying a real building, where dehumidification is performed by cooling coils.

With regard to the controller synthesis, the problem formulation could also include the damper opening fraction β as a decision variable. This will allow to obtain the maximum benefits from the outside weather predictions. For instance, free cooling or heating, which is a method of using the external air conditions to reduce the mechanical heat transfer of the HVAC system.

We also suggest to investigate the possibility to linearize the system. For instance, by the convexification method proposed in [12], or by a scheduled linearized MPC, in which the linear

model is the result of the linearization around several operating points, [8]. The availability of a linear system allows to simplify the proof for stability and robustness. Those subjects are complex for nonlinear systems and have not been discussed in this work.

The problem formulation could also be extended to several zones, where a distributed control method could be used to decompose the problem in a set of sub-problems with the coupling constraints from the air conditioning system. With the increasing complexity in the building model, computing the predictive controller action might become computationally expensive. And even though the time for solving the nonlinear MPC can be considered to be a nonrestrictive factor for the slow dynamics of the system, a significant increase in the number of zones will amount more computational time. Thus, this can be overcome by the distributed control scheme and a linear model of the system.

Appendix A

Psychrometrics

This appendix describes the psychrometrics of the air, where we explain basic concepts regarding the properties and processes of moist air relevant to the HVAC system under study. Herein, moist air is defined as a mixture of dry air and water vapor. Its psychrometric analysis is commonly used in HVAC systems to study, size and assess the performance of air conditioning systems in buildings, [25].

A-1 Properties of the air

The properties presented next are concepts used throughout this thesis project. These concepts and formulas were taken from [38, 39].

A-1-1 Dry-Bulb temperature

It is the temperature of the air, which can be measured by a thermometer freely exposed to the air that is shielded from radiation and moisture. This temperature is referred to as dry since the air moisture content will not cause variations in temperature.

A-1-2 Vapor pressure

It is the pressure exerted by vapor above a surface of water. With relevance to the calculation of humidity, the pressure of air at saturation e'_w and the saturation vapor pressure of moist are e_w are presented next.

Saturation vapor pressure

It is the pressure e'_w at which the process has reached an equilibrium with no change in either vapor pressure or density. We denote the saturation vapor pressure in the pure phase by e'_w,

and it is given as:

$$e'_w = 6.112 \exp\left(\frac{17.62T}{243.12+T}\right) \tag{A-1}$$

where e'_w saturation vapor pressure expressed in [hPa], and T the air temperature in [°C].

Saturation vapor pressure of moist air

This pressure e_w is expressed as the following product:

$$\begin{aligned} e_w(P,T) &= f(P)e'_w(T) && \text{(A-2a)} \\ f(P) &= 100(1.0016 + 3.15\times10^{-6}P - 0.074P^{-1}) && \text{(A-2b)} \end{aligned}$$

where e_w is the saturation vapor pressure of moist air [Pa], T is the air temperature in [°C], P is the barometric pressure in [hPa] ($P = 1013.25$ [hPa]), and $f(P)$ [Pa] is a constant parameter assuming the barometric pressure P is constant.

A-1-3 Humidity ratio

This property of the air denoted by W corresponds to the mass of water vapor m_v in a unit volume of air V. It is given as:

$$W = \frac{m_v}{V} \tag{A-3}$$

where m_v can be expressed in [g] of water vapor, and V in [kg] of dry air. Here, to derive (A-6) we introduce the law of perfect gases, which is given as:

$$eV = m_v R_v T \tag{A-4}$$

where, e [Pa], V [m^3], T [°K], and m_v [kg] are the air actual pressure, volume, temperature, and mass, and R_v is a constant equal to 461 [JKg^{-1}°K^{-1}]. From (A-4), we arrive to the expression $\frac{m_v}{V} = \frac{e}{R_v T}$, which is replaced in (A-3) and yields to:

$$W = \frac{e}{R_v T}\ \left[\frac{\text{kg}}{\text{m}^3}\right] \tag{A-5}$$

Since the units for mass in our system have been defined in kg, we multiply the denominator of (A-5) by the density of the air ρ_a, which yields to:

$$W = \frac{e}{R_v T \rho_\text{a}}\ \left[\frac{\text{kg}}{\text{kg}}\right] \tag{A-6}$$

We can replace in (A-6) the actual vapor pressure $e = \frac{e_w RH}{100}$ from (A-8), (A-1) and (A-2). The following relation is found:

$$W = \frac{6.112 f(P)}{R_v \rho_{\mathrm{a}}} \frac{RH}{T + 273} \exp\left(\frac{17.62T}{243.12 + T}\right) \left[\frac{\mathrm{kg}}{\mathrm{kg}}\right] \tag{A-7}$$

where W is the air humidity ratio [$\mathrm{kg_w kg_a^{-1}}$], $f(p)$ is a constant function of the barometric pressure P [Pa], ρ_{a} the density of the air [$\mathrm{kg_a m^{-3}}$], T the air temperature [°C], and RH the relative humidity [%].

A-1-4 Relative Humidity

This air property corresponds to the ratio of the actual amount of water vapor in the air to the amount it could hold when saturated. It is expressed as a percentage or the ratio of the actual vapor pressure e to the saturation vapor pressure expressed e_w as a percentage. The expression of the relative humidity RH is given by:

$$RH = 100 \frac{e}{e_w} \tag{A-8}$$

From (A-7), we can find RH:

$$RH = \frac{R_v \rho_{\mathrm{a}}}{6.112 f(P)} (T + 273) W \exp\left(\frac{-17.62T}{243.12 + T}\right) [\%] \tag{A-9}$$

where RH is the relative humidity [%], $f(p)$ is a constant function of the barometric pressure P [Pa], ρ_{a} the density of the air [$\mathrm{kg_a m^{-3}}$], T the air temperature [°C], and W the humidity ratio [$\mathrm{kg_w kg_a^{-1}}$].

A-1-5 Dew-point temperature

It is also known as saturation temperature T_{d} and corresponds to the temperate at which the water vapor of the air condensates. T_{d} is described by the approximation, [40]:

$$T_{\mathrm{d}} = T - \frac{100 - RH}{5} \tag{A-10}$$

where T [°C] is the temperature and RH [%] the relative humidity.

A-1-6 Enthalpy

It corresponds to the total heat content of the air, which entails latent and sensible heat. The enthalpy h is expressed as follows:

$$h = c_{\mathrm{a}} T + h_{\mathrm{wv}} W$$

where $c_{\mathrm{a}} = 1.006$ [$\mathrm{kJkg_a^{-1}{}^{\circ}C^{-1}}$] is the specific heat coefficient of the air , $h_{\mathrm{wv}} = 2454$ [$\mathrm{kJkg_{wv}^{-1}}$] is the specific heat of water vapor, T [°C] the temperature and W [$\mathrm{kg_w kg_a^{-1}}$] the humidity ratio.

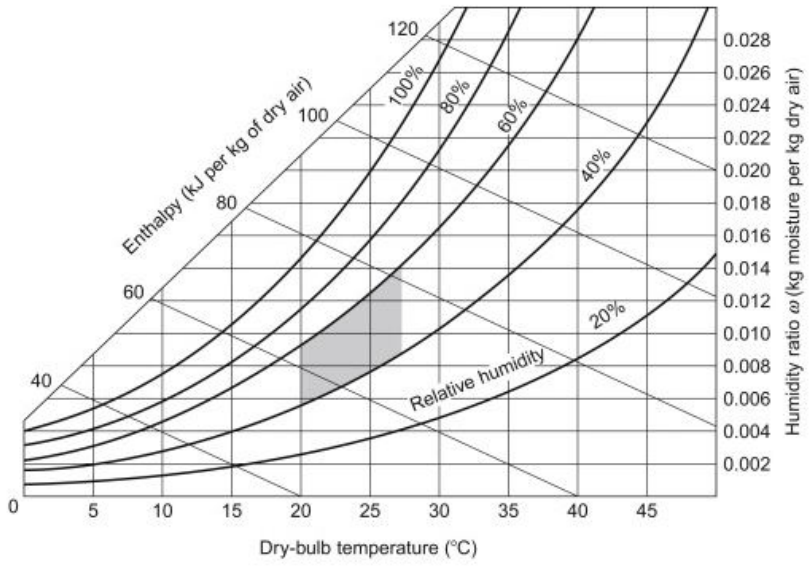

Figure A-1: Psychrometric chart, [6]

A-2 Psychrometric chart

It is a visual aid that shows the relations of the properties of the air, Figure A-1. In HVAC systems, this chart is a standard tool to visualize, design and analyze the air-conditioning processes and energy changes that experiences the air, [25].

The chart Figure A-1 shows the properties of moist air in terms of dry-bulb temperature, relative humidity, humidity ratio and enthalpy. The knowledge of two of these properties are sufficient to identify the phase of the air, [6].

In Figure A-1 the dry-bulb temperature is graphically represented by vertical lines, the humidity ratio by horizontal lines, the enthalpy by oblique lines, and the relative humidity by the curves. Herein, when the air has reached 100% RH, the curve is called the saturation curve. The dew-point temperatures of the air lay over this curve.

A-3 Psychrometric processes

This section describes the processes analyzed throughout this thesis project.

A-3-1 Sensible heating or cooling

This process is characterized by an increase or decrease in the temperature of air without changing its humidity ratio. This movement in the chart corresponds to a horizontal variation along the humidity ratio lines. For instance, increasing the temperature from **point 2** to **point 3** as shown in Figure A-2. Here, the initial temperature of 60°C is increased horizontally (no humidity ratio variation) until 70°C. The readings provided from the chart are a variation of

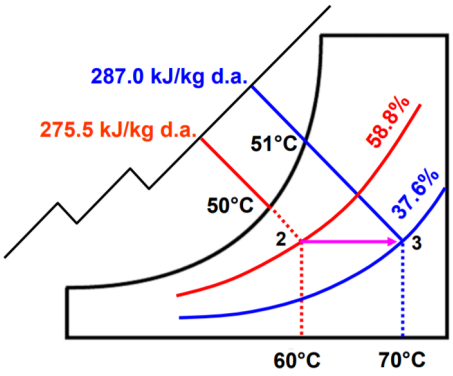

Figure A-2: Heating process movement in the Psychrometric chart, [7]

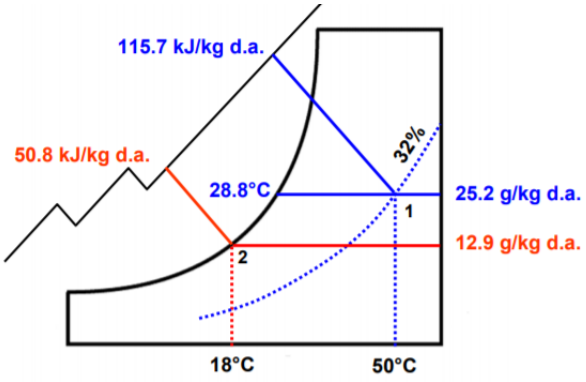

Figure A-3: Cooling and dehumidifying process movements in the Psychrometric chart, [7]

enthalpy from 275.5 $kJkg_a^{-1}$ to 287.0 $kJkg_a^{-1}$, which are represented by the diagonal blue and red lines. The readings of the relative humidity are 58.8% and 37.6%, and they are described by the curvy red and blue lines at each point, [7].

A-3-2 Cooling and dehumidifying

This process involves the removal of moisture from the air. Removal that happens when the air has reached a temperature less than the dew-point. In Figure A-3, the air is cooled from **point 1** to **point 2**, where there exists a decrease of the humidity ratio from 25.2 $g_w kg_a^{-1}$ to 12.9 $g_w kg_a^{-1}$ and also a decrease of temperature from 50 °C to 18 °C. The readings from the chart allows to identify the dew-point temperature given by 28.8 °C, the enthalpies of 115.7 $kJkg_a^{-1}$ and 50.8 $kJkg_a^{-1}$ and the relative humidity 32% and 100% at each point. **Point 2** lays over the saturation line that corresponds to the relative humidity of 100%, [7].

Appendix B

Model Predictive Control (MPC)

B-1 Principles

This control strategy comprises a model-based algorithm that computes a control signal by minimizing an objective function subject to a set of constraints. To explain it, we consider the system (B-1), where f and h are smooth functions of x and u, [41].

$$x(k+1) = \quad f(x(k), u(k)) \tag{B-1a}$$
$$y(k) = \quad h(x(k), u(k)) \tag{B-1b}$$

MPC considers the prediction of the system over the period $[k+1, k+N_\mathrm{p}]$, where N_p corresponds to the prediction horizon and k to the current sample step, Figure B-1. From (B-1), we can obtain the estimates $\hat{y}(k+j|k)$ based on the state $x(k)$ at time step k and the future input sequence $u(k), u(k), \cdots, u(k+j-1)$. This leads to:

$$\hat{y}(k+j|k) = F_j(x(k), u(k), u(k), \cdots, u(k+j-1)),\ j = 1, \cdots, N_\mathrm{p} \tag{B-2}$$

By defining the vectors:

$$\tilde{u}(k) = \left[u^\top x(k) \ \cdots \ u^\top(k)x(k+N_\mathrm{p}-1)\right] \tag{B-3a}$$
$$\tilde{y}(k) = \left[\hat{y}^\top x(k+1|k) \ \cdots \ \hat{y}^\top(k)x(k+N_\mathrm{p}|k)\right], \tag{B-3b}$$

The following equation is obtained:

$$\tilde{y}(k) = F(x(k), \tilde{u}(k)) \tag{B-4}$$

B-2 Cost function and constraints

A cost function $J(k)$ is associated to the goals required, which corresponds to a function minimized over all future possible input sequences subject to the constraints imposed.

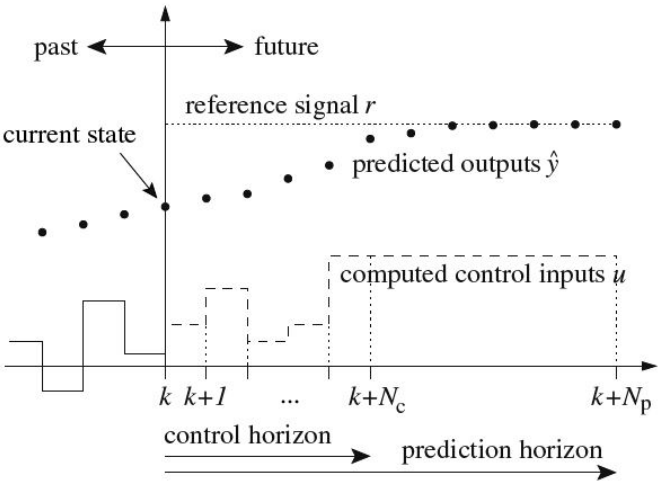

Figure B-1: MPC strategy, adapted from [8]

B-3 Prediction horizon

The aforementioned problem is solved over the time horizon given by the prediction horizon, N_p. This term corresponds to the number of future time intervals, in which the open-loop control problem is evaluated and optimized.

B-4 Control horizon

To reduce the problem, a control horizon N_c is introduced, which means that after step $k + N_\mathrm{c} - 1$ the input u is held constant.

$$u(k + j) = u(k + N_\mathrm{c} - 1), \text{ for } j = N_\mathrm{c}, \cdots, N_\mathrm{p} - 1 \tag{B-5}$$

B-5 Receding horizon principle

The optimization problem defined by the objective function $J(k)$ and the constraints results in the optimal input trajectory $\boldsymbol{u}$. Only the first control input calculated is implemented to (B-1). Time is shifted on step, and the model is updated from the measurements. A new optimization is performed starting from the new measurements, and again the first optimal input is implemented. Until the end of the simulation, the control signal is recursively recalculated in the next samples using new measurements following the receding horizon principle.

Appendix C

Building characteristics

This appendix describes the characteristics of the building analyzed in the numerical case of study from Section 3-5. The parameters from Section C-2 are taken from [21], and the values from Section C-3 have been inspired by the work found in [42]. At the end of this appendix, we also include the weather conditions, which were taken from [35].

C-1 General considerations

The building corresponds to a high occupancy building (zone) of the following physical characteristics:

$$A_{\text{wall}} = 180[\text{m}^2],\ \ A_{\text{floor}} = 200[\text{m}^2],\ \ A_{\text{win}} = 50[\text{m}^2],\ \ V_{\text{z}} = 600[\text{m}^3],$$

The building thermal capacitance $C_{\text{z}} = 1.4 c_{\text{a}} \rho_{\text{a}} V_{\text{z}}$ has been chosen such that the capacitance of furnishings and zone contents are taken into account. The air mass in the zone is $M_{\text{z}} = \rho_{\text{a}} V_{\text{z}}$.

C-2 Air properties coefficients

Specific heat coefficient of air	$c_{\text{a}} =$	$1.006\ [\text{kJkg}_{\text{a}}^{-1\circ}\text{C}^{-1}]$
Latent heat of vaporization of water vapor	$h_{\text{wv}} =$	$2454\ [\text{kJkg}_{\text{wv}}^{-1}]$
Density of air	$\rho_{\text{a}} =$	$1.205\ [\text{kg}_{\text{a}}\text{m}^{-3}]$

C-3 Factors and coefficients

Convection factor - windows	$cf_{\text{win}} =$	$1.012\,[-]$
Convection factor - equipment	$cf_{\text{eq}} =$	$0.23\,[-]$
Convection factor - lighting	$cf_{\text{light}} =$	$0.08\,[-]$
Convection factor - person	$cf_{\text{per}} =$	$0.02\,[-]$
Solar Gain factor	$SGF =$	$0.5\,[-]$
Thermal transmittance - wall	$U_{\text{wall}} =$	$0.62\,[\text{Wm}^{-2\circ}\text{K}^{-1}]$
Sensible heat rate - person	$\dot{Q}_{\text{per}} =$	$80\,[W]$
Moisture rate - person	$H_{\text{person}} =$	$0.06\,[\text{kg}_{\text{w}}\text{h}^{-1}]$
Heat flux - Equipment	$q_{\text{eq}} =$	$3.2\,[\text{Wm}^{-2}]$
Heat flux - Lighting	$q_{\text{light}} =$	$4.5\,[\text{Wm}^{-2}]$

C-4 Disturbances prediction

Figure C-1 and C-2 present the sensible $\dot{Q}_{\text{int}}$ and latent loads $\dot{W}_{\text{int}}$, and the occupancy profile N_{per} used for the simulations. The two former were obtained using the equations and principles explained in Chapter 2. The number of people is a scaled version of [36]. The prediction correspond to August 29,16 5:00 to August 30,16 10:00 and September 13,16 5:00 to September 14,16 10:00.

C-5 Weather conditions

The weather conditions were taken from [35]. From which the hourly weather data was converted to fifteen minutes data by linear interpolation. Figure C-3 and C-4 show the outside temperature T_{oa}, humidity ratio W_{oa} and solar radiation I_o in fifteen minutes intervals of August 29, 2016 5:00 to August 30, 2016 10:00 and September 13, 2016 5:00 to September 13, 2016 10:00 and.

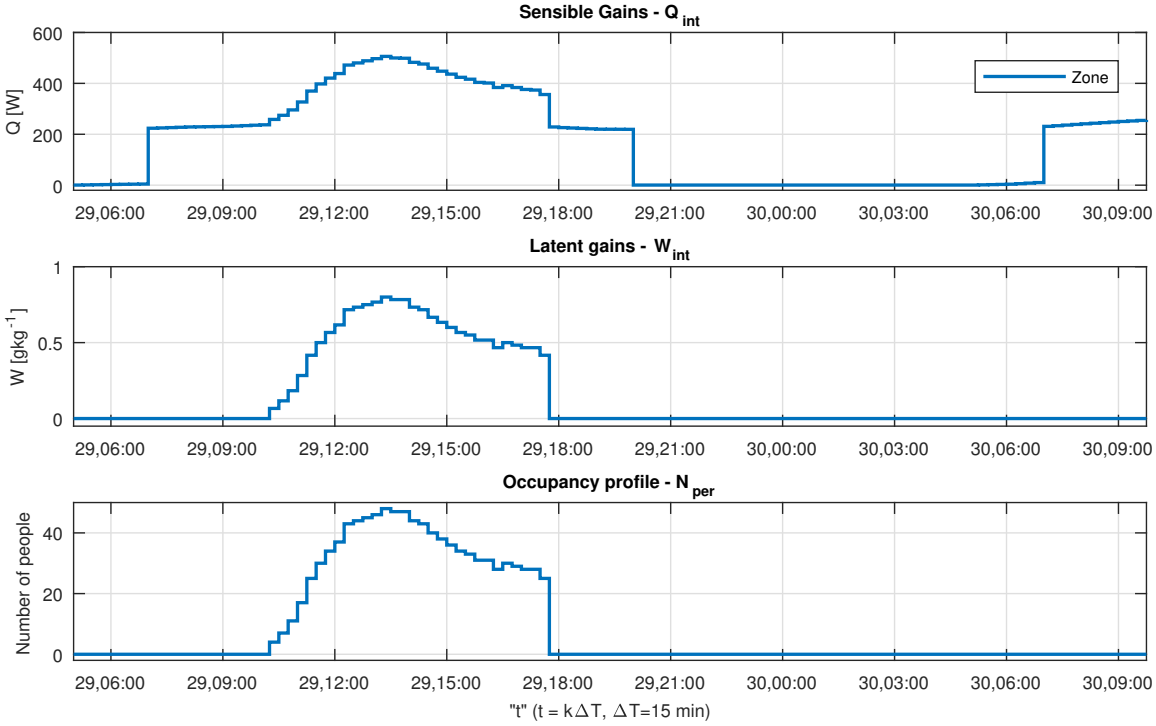

Figure C-1: Building (zone) disturbances August 29,16 5:00 to August 30,16 10:00

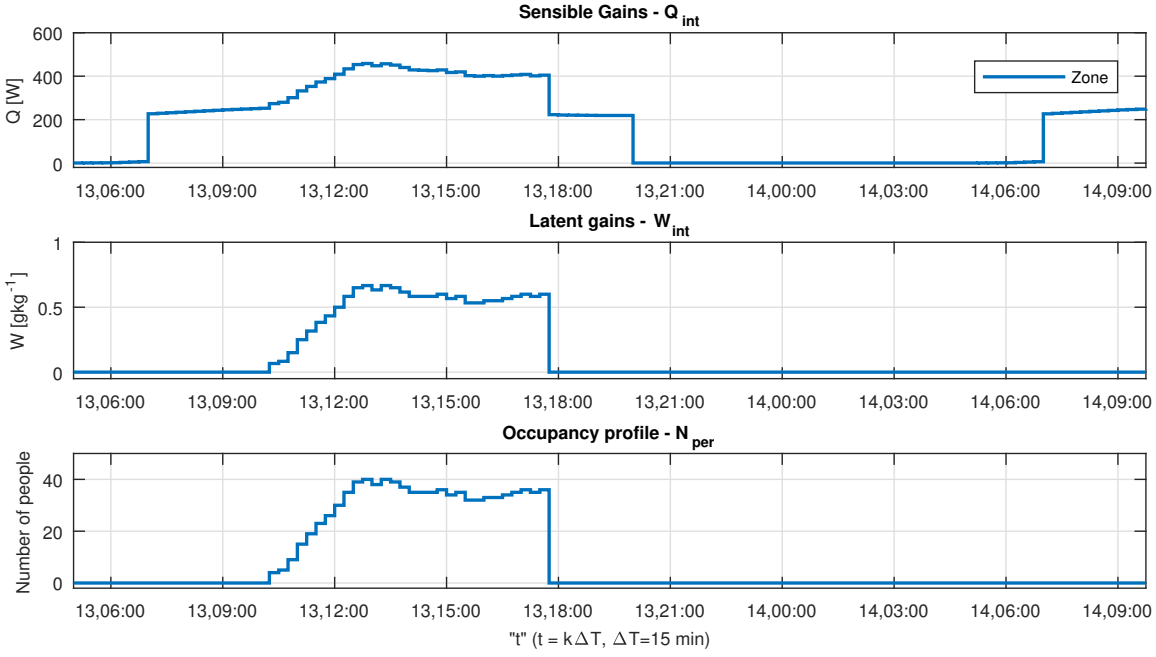

Figure C-2: Building (zone) disturbances September 13,16 5:00 to September 14,16 10:00

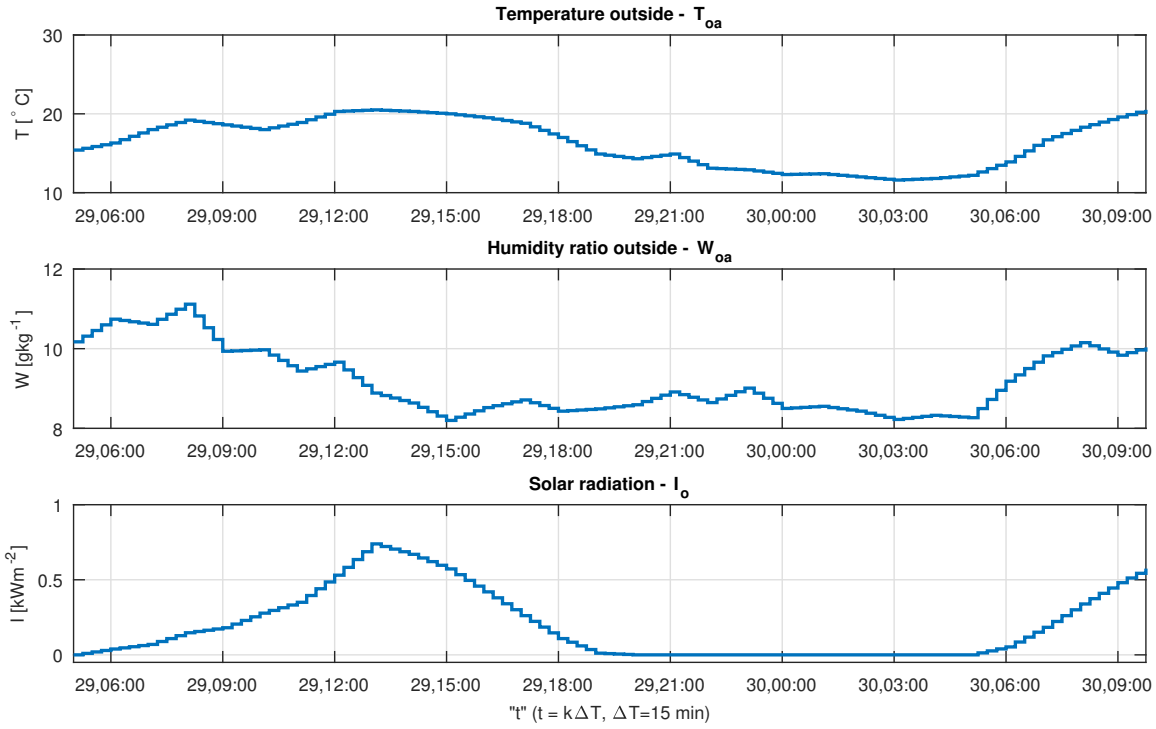

Figure C-3: Weather conditions. From August 29 5:00 am until August 30 10:00 am, 2016

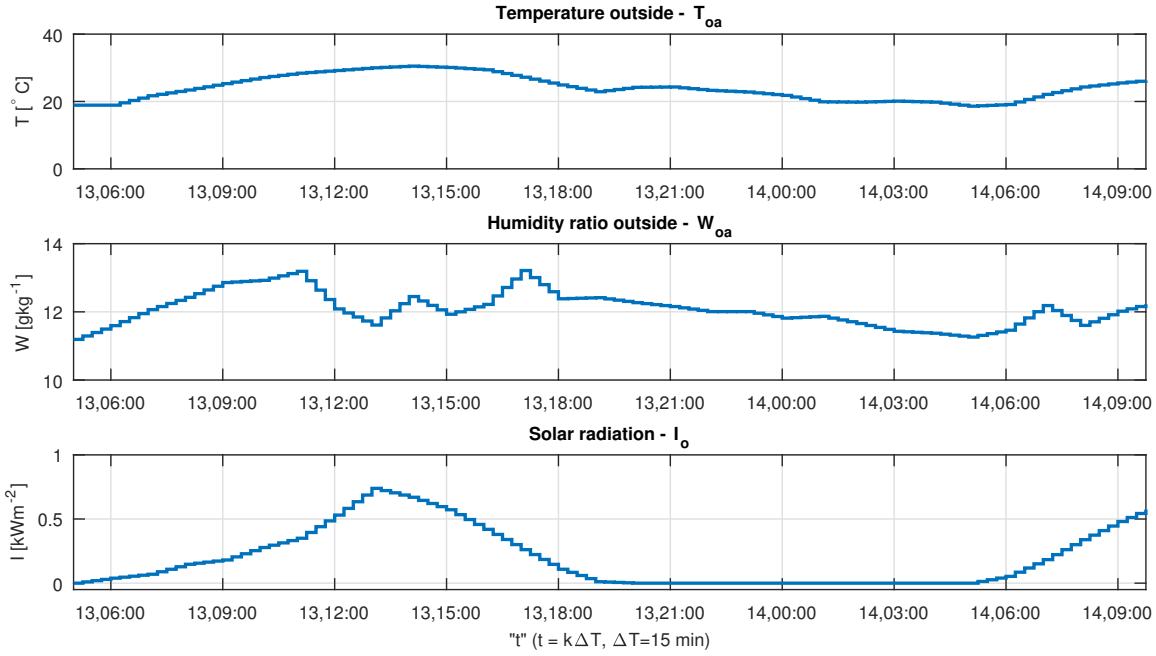

Figure C-4: Weather conditions. From September 13 5:00 am until September 14 10:00 am, 2016

Bibliography

[1] International Energy Agency (ISA), "Heating in buildings - tracking clean energy progress." https://www-iea-org.tudelft.idm.oclc.org/tcep/buildings/heating/, 2018. [Online; accessed 21-Nov-2018].

[2] W. Zeiler, K. Gvozdenović, K. de Bont, and W. Maassen, "Toward cost-effective nearly zero energy buildings: The Dutch situation," *Science and Technology for the Built Environment*, vol. 22, no. 7, pp. 911–927, 2016.

[3] A. Kusiak, F. Tang, and G. Xu, "Multi-objective optimization of HVAC system with an evolutionary computation algorithm," *Energy*, vol. 36, no. 5, pp. 2440 – 2449, 2011.

[4] EDSLTas, "Heat Transfer Mechanisms in Buildings." http://edsl.myzen.co.uk/manuals/Building%20Simulator/SchematicRepresentationofHeatTransfermechanisminaBuilding.htm. [Online; accessed 29-Oct-2018].

[5] P. Wilson and H. A. Mantooth, "Chapter 3 - design analysis," in *Model-Based Engineering for Complex Electronic Systems*, pp. 47 – 48, Oxford: Newnes, 2013.

[6] R. T. Balmer, "Appendix D - Thermodynamic Charts," in *Modern engineering thermodynamics-textbook with tables booklet*, p. 69, Academic Press, 2011.

[7] P. Peralta, "The psychrometric chart - theory and application," in *Proceeding SWST 48th Annual Convention*, pp. 1–50, Society of Wood Science and Technology, Jun 2005.

[8] E. Camacho, C. Bordons, and C. Alba, *Model Predictive Control*, pp. 1–10 – 249–282. Advanced Textbooks in Control and Signal Processing, Springer London, 2004.

[9] X. Xu, Z. Zhong, S. Deng, and X. Zhang, "A review on temperature and humidity control methods focusing on air-conditioning equipment and control algorithms applied in small-to-medium-sized buildings," *Energy and Buildings*, vol. 162, pp. 163 – 176, 2018.

[10] M. Y. Lamoudi, *Distributed model predictive control for energy management in buildings*. PhD thesis, Université de Grenoble, 2012.

[11] N. R. Patel, M. J. Risbeck, J. B. Rawlings, M. J. Wenzel, and R. D. Turney, "Distributed economic model predictive control for large-scale building temperature regulation," in *American Control Conference (ACC)*, pp. 895–900, Jul 2016.

[12] Z. Wang, G. Hu, and C. J. Spanos, "Distributed model predictive control of bilinear HVAC systems using a convexification method," in *11th Asian Control Conference (ASCC)*, pp. 1608–1613, Dec 2017.

[13] A. Kelman and F. Borrelli, "Bilinear Model Predictive Control of a HVAC System Using Sequential Quadratic Programming," *18th IFAC World Congress Proceedings Volumes*, vol. 44, no. 1, pp. 9869 – 9874, 2011.

[14] B. Dong and K. Lam, "A real-time model predictive control for building heating and cooling systems based on the occupancy behavior pattern detection and local weather forecasting," *Building Simulation*, vol. 7, pp. 1–18, Feb 2014.

[15] J. Rehrl, D. Schwingshackl, and M. Horn, "Model Predictive Control of Temperature and Humidity in Heating, Ventilating and Air Conditioning Systems," *IFIP Advances in Information and Communication Technology*, vol. 443, pp. 285–295, Nov 2014.

[16] J. Mei and X. Xia, "Energy-efficient predictive control of indoor thermal comfort and air quality in a direct expansion air conditioning system," *Applied Energy*, vol. 195, pp. 439 – 452, 2017.

[17] L. Jingyun and L. Ping, "Temperature and humidity control with a model predictive control method in the air-conditioning system," in *International Conference on Advanced Mechatronic Systems (ICAMechS)*, pp. 408–412, Dec 2017.

[18] H. Xu, Z. Zhai, K. Wang, S. Ren, and H. Wang, "Multiobjective distributed model predictive control method for facility environment control based on cooperative game theory," *Turkish Journal of Electrical Engineering & Computer Sciences*, vol. 25, no. 5, pp. 4160–4171, 2017.

[19] R. J. Van Ooteghem, "Optimal control design for a solar greenhouse," *IFAC Proceedings Volumes*, vol. 43, no. 26, pp. 304–309, 2010.

[20] C. Li, X. Zhang, and S. Chung, "Temperature and humidity control for an automobile during heating period," in *Chinese Control and Decision Conference (CCDC)*, pp. 2577–2582, May 2011.

[21] H. Struchtrup, "Chapter 3 - the first law of thermodynamics," in *Thermodynamics and energy conversion*, pp. 33 – 44, Springer, 2014.

[22] E. Walker and R. J. Blaen, "10 - Industrial boilers," in *Plant Engineer's Reference Book* (D. A. Snow, ed.), pp. 10–1 – 10–28, Oxford: Butterworth-Heinemann, second ed., 2002.

[23] C. J. Roos, *Principles of Heat Transfer: Supplement to Heat Transfer Product Reviews*, pp. 1–6. Washington State University Extension Energy Program, 2008.

[24] A. Moser, "Buildings and heat transfer." http://www.thermopedia.com/es/content/603/, 2011. [Online; accessed 04-Jul-2018].

[25] C. Ghiaus, "Linear algebra solution to psychometric analysis of air-conditioning systems," *Energy*, vol. 74, pp. 555 – 566, 2014.

[26] M. Maasoumy and A. Vincentelli, "Total and Peak Energy Consumption Minimization of Building HVAC Systems Using Model Predictive Control," *Design Test of Computers, IEEE*, vol. 29, pp. 26–35, Aug 2012.

[27] A. Kelman, Y. Ma, and F. Borrelli, "Analysis of local optima in predictive control for energy efficient buildings," in *50th IEEE Conference on Decision and Control and European Control Conference*, pp. 5125–5130, Dec 2011.

[28] G.-Y. Jin, W.-J. Cai, Y.-W. Wang, and Y. Yao, "A simple dynamic model of cooling coil unit," *Energy Conversion and Management*, vol. 47, no. 15, pp. 2659 – 2672, 2006.

[29] H. Satyavada and S. Baldi, "An integrated control-oriented modelling for HVAC performance benchmarking," *Journal of Building Engineering*, vol. 6, pp. 262 – 273, 2016.

[30] E. van Vliet, "Flexibility in heat demand at the TU Delft campus smart thermal grid with phase change materials," Master's thesis, Delft University of Technology, the Netherlands, 2013.

[31] S. Baldi, S. Yuan, P. Endel, and O. Holub, "Dual estimation: Constructing building energy models from data sampled at low rate," *Applied Energy*, vol. 169, pp. 81 – 92, 2016.

[32] S. Li, J. Joe, J. Hu, and P. Karava, "System identification and model-predictive control of office buildings with integrated photovoltaic-thermal collectors, radiant floor heating and active thermal storage," *Solar Energy*, vol. 113, pp. 139 – 157, 2015.

[33] P. O. M. Scokaert and J. B. Rawlings, "Feasibility issues in linear model predictive control," *AIChE Journal*, vol. 45, pp. 1649 – 1659, Aug 1999.

[34] E. C. Kerrigan and J. M. Maciejowski, "Soft constraints and exact penalty functions in model predictive control," in *UKACC International Conference (Control)*, pp. 1–6, 2000.

[35] Koninklijk Nederlands Meteorologisch Instituut, "Weather forecasting and monitoring of weather, climate, air quality and seismic activity." https://cdn-knmi-nl.tudelft.idm.oclc.org/knmi/map/page/klimatologie/gegevens/uurgegevens/uurgeg_240_2011-2020.zip. [Online; accessed 02-Feb-2019].

[36] Van Gogh Museum, "Occupancy profile data." unpublished, 2016.

[37] J. Lofberg, "YALMIP : A toolbox for modeling and optimization in MATLAB," in *IEEE International Conference on Robotics and Automation*, pp. 284–289, Sep. 2004.

[38] American Society of Heating and Refrigerating and Air-Conditioning Engineers (ASHRAE), "Chapter 1 - psychrometrics," in *ASHRAE handbook: Fundamentals*, pp. 1.1 – 1.17, 2017.

[39] World Meteorological Organization, "Annex 4.B - Formulae for the computation of measures of humidity," in *Guide to Meteorological Instruments and Methods of Observation*, vol. 8, p. I4.29, Jan 2008.

[40] M. Lawrence, "The Relationship between Relative Humidity and the Dewpoint Temperature in Moist Air: A Simple Conversion and Applications," *Bulletin of the American Meteorological Society*, vol. 86, pp. 225–233, Feb 2005.

[41] B. De Schutter, W. Heemels, and A. Bemporad, "Modeling and control of hybrid systems," *Lecture notes of the DISC course*, pp. 1–170, 2015.

[42] W. W. Ananduta, "Distributed Energy Management in Smart Thermal Grids with Uncertain Demands," Master's thesis, Delft University of Technology, the Netherlands, 2016.

Glossary

List of Acronyms

HVAC	Heating, Ventilation and Air Conditioning
MPC	Model Predictive Control
AHU	Air Handling Unit
PID	Proportional, Integral, Derivative
EPBD	Performance of Building Directive
ISA	International Society of Automation
VAV	Variable Air Volume
MIMO	Multiple-Input Multiple-Output
BEMS	Building Energy Management System
ASHRAE	American Society of Heating and Refrigerating and Air-Conditioning Engineers
WMO	World Meteorological Organization
KNMI	Koninklijk Nederlands Meteorologisch Instituut
SQP	Sequential Quadratic Programming
ISA	International Energy Agency

List of Symbols

ρ	Density [kgm^{-3}]
h_{wv}	Latent heat vaporization of water vapor [$\mathrm{kJkg}_{\mathrm{wv}}^{-1}$]

$\dot{m}$	Mass flow rate [$m^3 s^{-1}$]
$\dot{Q}$	Heat transfer rate [kW]
c_a	Specific heat coefficient of air[$kJkg_a^{-1}{}^{\circ}C^{-1}$]
h	Enthalpy [$kJkg_a^{-1}$]
Q	Heat energy [kWh]
q	Heat flux [kWm^{-2}]
T	Temperature [°C]
V	Volume [m^3]
W	Humidity ratio [$kg_w kg_a^{-1}$]
A	Area [m^2]
C	Thermal capacitance [$kJ^{\circ}K^{-1}$]
U	Thermal transmittance [$Wm^{-2}{}^{\circ}K^{-1}$]